Journal of Constructional Steel Research 217 (2024) 108627

Contents lists available at ScienceDirect

Journal of Constructional Steel Research

journal homepage: www.elsevier.com/locate/jcsr

Probabilistically modelled geometrical imperfections for reliability analysis of vertically loaded steel frames

Daniel Jindra *, Zdeněk Kala, Jiří Kala

Faculty of Civil Engineering, Brno University of Technology, Veveří 331/95, 602 00 Brno, Czech Republic

ARTICLE INFO

Keywords:
Multi-story steel frames
Initial geometric imperfection
Erection tolerances
Correlations
First order reliability method
Geometrically nonlinear analysis

ABSTRACT

The article explores the stochastic modelling of 3D steel frames under static vertical load, with a main focus on random initial geometrical imperfections. The random input parameters for initial geometrical imperfections are derived from the tolerance criteria in accordance with European standard. In order to derive statistical parameters from the corresponding standard tolerances, two methods noted as #RSS (random storey sway) and #RSP (random storey position) have been utilized and compared. Both of these methods are used along with the first-order reliability method (FORM) and the advanced finite element method (FEM) – geometrically and materially nonlinear imperfect analysis (GMNIA) to numerically analyse several geometries of steel frame structures. Ultimate resistances of these structures are monitored and basic sensitivity studies are conducted. The results are also compared with the deterministic approach of the European standard. The stochastic approach of the FORM to estimate the ultimate resistance of steel frame structures serves as a verification tool of the classic, in engineering praxis widely used, deterministic approach. This study provides useful provisions for the advanced numerical analyses of steel frames of various geometries. Additionally, the estimations of ultimate resistance by the deterministic European standard approach is verified for selected frame geometries.

1. Introduction

For the analysis of steel frame structures, it is crucial to consider initial imperfections that can influence their load-bearing capacity [1]. These imperfections can be categorized into three main groups: geometrical imperfections, material imperfections, and structural imperfections [2,3]. Geometrical imperfections, resulting from manufacturing and erection tolerances, present as local (bow) and global (out-of-plumb) forms. Although commonly modelled as worst-case scenarios to amplify destabilizing load effects, such conservative estimations can lead to uneconomical designs, as noted by Shayan et al. [4]. The present study introduces stochastic methods for modelling initial geometrical imperfections in 3D steel frames, focusing on global and local random imperfections, while excluding cross-sectional geometrical imperfections.

In certain cases, the initial imperfections have been neglected, e.g. in the study on steel-concrete composite frame structures [5], or analysis of the progressive collapse of post-tensioned steel frames [6], where the numerical results were considered as satisfactory given the initial imperfections in the test specimens. Initial imperfections were not considered as a major concern in numerical and experimental analysis of coupled steel-concrete composite wall-frame structures [7], or in detailed analysis of floor deck connections [8]. Segura et al. [9] neglected the explicit modelling of geometric imperfections, studying their minimal influence on specific frame types. This conclusion was supported by earlier validation of the model against experimental results of frames exposed to fire [10].

However, for other types of structures, the effect of initial geometric imperfection is not negligible, and should be considered. This is also mentioned in several standards, e.g. Eurocode for steel structure design [11]. For example, Chan et al. [12] have compared two methods to introduce the initial geometrical imperfections. The effects of initial geometric imperfections applied on the 2D braced portal frames are more significant compared to the unbraced 2D frames, as the bracings resist lateral movement, but cannot reduce the bow imperfection leading to the P–δ effect. Systematic method to evaluate the appropriate "equivalent initial imperfections" that need to be incorporated in the second-order global elastic analysis of in-plane frame structures are also discussed by Goncalves et al. [13]. Geometrical imperfections are often required to be considered for slenderer members, as recently

* Corresponding author.
E-mail address: Daniel.Jindra@vut.cz (D. Jindra).

https://doi.org/10.1016/j.jcsr.2024.108627
Received 28 November 2023; Received in revised form 29 February 2024; Accepted 18 March 2024

investigated for welded box-sections members by Radwan et al. [14]. Piątkowski [15] recommended to use the complex numerical models including imperfect elements of the bracing system and to use geometrically nonlinear analysis in order to determine the influence of assumed geometric imperfections on all elements, bracings and connections of the analysed structure.

Previous studies have extensively addressed the structural analysis of steel constructions with initial geometrical imperfections. For instance, Clarke et al. [16] followed Australian design specifications, Liew et al. [17] modelled inelastic behaviour of frames, and Shayan et al. [4] introduced a method for modelling these imperfections using eigenmodes for 2D frames. Current research includes imperfection scaling based on strain energy and the entropy method, as discussed by Kala [18,19] and the use of terrestrial laser scanners to measure imperfections, as explored by Chacón et al. [20].

Several approaches address initial geometrical imperfections in steel frame analysis:

- Scaling of the elastic buckling mode (EBM), where the first buckling mode of linear elastic buckling analysis (of a perfect structure) is scaled to approximate the imperfect geometry [21]. This method is still being improved. Aguero et al. extended EBM to non-uniform cross-sections [22]. However, EBM poses risks if first and second critical loads coincide [23]. Also, plastic deformations may deviate from the elastic buckling mode. A plastic second-order analysis reveals the final failure shape, which might be also scaled to determine the initial imperfect geometry [24]. However, this approach might be overly conservative, as the collapse geometry is induced at the initiation of the structural analysis.
- Notional horizontal forces method (NHF) permitted by design standards such as the European standard 1993-1-1 [11], replaces the sway imperfection effects with equivalent horizontal forces, as utilized by Liew et al. [25].
- Member stiffness reduction, suggested by Kim [26], who reduced the elastic modulus to 0.85E to reflect the effects of geometric imperfection. However, this value lacks full probabilistic validation [4].
- Direct modelling of the initial geometrical imperfection, used e.g. by Chan [12] and presented also in this study, where the nodal coordinates of the finite element mesh are offset from the original position. This also enables the integration of probabilistic methods, discussed in relation to 3D frame structures.

The statistical modelling of imperfections is critical for verifying equivalent imperfection formulas and their application in frame calculations as per various standards, a point emphasized by Machowski et al. [27]. Currently, the most effective modelling of geometric imperfections is achieved through probabilistic methods, which can address the complexity of 3D structures, including the patterns of imperfections [4]. Probabilistic methods are often compared with deterministic approach, as for example in case of analysis of the steel-concrete composite floor progressive collapse by Ding et al. [28], who highlighted the importance of modelling uncertainties. Probabilistic modelling is the ultimate tool for cases, where the structural reliability is based on experimentally determined input parameters (stochastic values), where the standardized design approach is not yet fully developed or needs to be verified by probabilistic methods. The aim of this study is to verify the ultimate resistances of several geometrically imperfect steel frame structures through stochastic analyses, directly addressing the problems of uneconomical designs under deterministic assumptions as highlighted by both the EN 1993-1-1 [11] standards and Shayan et al. [4].

European standard EN 1990 [29] recognizes two main classes of reliability methods:

- Full probabilistic methods, which give in principle correct answers to the reliability problems, but are seldom used in the calibration of design codes due to frequent lack of statistical data.
- First order reliability method (FORM), which for most structural applications lead to sufficiently accurate results [29].

In the European standard EN 1990 [29], the reliability design conditions are based on the FORM (first-order reliability method). FORM belongs to one of the most important methods for the evaluation of structural reliability, mainly in combination with methods of the advanced numerical analyses, e.g., the finite element method (FEM) as also discussed by Faber [30] or Zhao and Ono [31]. The concept of this FORM method (in more detail described in studies by Kala [32–34] and Jönsson [35]) allows the assumption of the Gauss probability density function (PDF) for load and structural resistance. Since the random variables for the description of the loading and the resistance are statistically uncorrelated, the resistance can be studied independently of the load. In this paper, FORM has been utilized to analyse the design ultimate resistance of various steel frames.

As several options to consider the initial geometrical imperfections are available, it is often required to conduct a comparison study of these methods considering the analysed structure, or to verify the utilized method to consider the initial geometrical imperfections. The study presented in this paper focuses on the stochastic modelling of initial geometrical imperfections in steel frame structures, which is considered to be the most rational of the available methods [4]. The results obtained using probabilistic methods could be valuable for verifying the other deterministic approaches in the global analysis of geometrically imperfect 3D steel frames.

Advanced numerical geometrically and materially nonlinear analyses with imperfections (GMNIA) using the ANSYS software [36] are conducted in order to determine the resistance of steel frames. Methods of numerical analyses of steel structures are widely used in engineering praxis and research, as these offer advanced insight in the structural response of complex geometries, as for example cable structures analysed by Chen et.al [37], where geometrical nonlinearities need to be considered.

In this paper, two approaches to define the initial geometrical imperfections are compared (described in the chapter 2 of this paper). The first one is simplified in accordance with EC3 [11] assumptions, expected to be more conservative as the defined imperfections are designed to be sufficiently safe. The second approach is probabilistic, using stochastic values of the input parameters along with the semi-probabilistic first-order reliability method (FORM), described in European standard EN 1990-1-1 [29]. The probabilistic approach, assumed to yield more realistic outcomes, utilizes statistical parameter values from EN 1090–2:2018 [38].

Due to the fact the standard defines criteria for two mutually dependent parameters (sways and also cumulative deviations of the floors relative to the base position), it is possible to consider two different, but complementary approaches for stochastic input parameters, as further described in the chapter 3 of this paper, noted as #RSS and #RSP for “random storey sway” and “random storey position” respectively. These two methods have been statistically verified in the previous study [39].

The numerical analyses detailed in chapters 4 and 5 lead to results, discussions, summaries and conclusions in chapters 6 through 9. This paper also provides useful information about the possible workflows, and recommendations of how to consider the mutual correlations between the random input parameters which determine the initial geometrical imperfections, in case these are derived based on tolerance criteria of the EN 1090–2:2018 [38].

2. Methods to determine the structural resistance of steel frames

The results based on two approaches to determine the structural resistance of steel frames are compared. The first, in accordance with EC3 [11] assumptions, utilizes all the input parameters as deterministic (chapter 2.1), hence, only single calculation per frame geometry is

conducted. In the second approach, the semi-probabilistic method along with stochastic input parameters is utilized (chapter 2.2), hence, sufficiently large number of calculations are required to be conducted in order to obtain data for statistical evaluation.

2.1. European standard assumptions; #EC3

In accordance with the chapter 5.3.2 of the EC3 [11], the global initial sway imperfections are defined by angle ϕ which is applied on the whole structure in one direction:

$$\phi = \phi_0 \alpha_h \alpha_m \tag{1}$$

where ϕ_0 is the basic value of 1/200, α_h is the reduction factor for height of the structure h (in meters):

$$\alpha_h = \frac{2}{\sqrt{h}}; \frac{2}{3} \leq \alpha \leq 1.0 \tag{2}$$

and α_m is the reduction factor for the columns in a row:

$$\alpha_m = \sqrt{0.5\left(1 + \frac{1}{m}\right)} \tag{3}$$

Where m is the number of columns in a row (including only those columns which carry a vertical load not <50% of the average value of the column in the vertical plane considered.

Design values of the initial bow imperfections are dependent on the buckling curve of the cross-section (Table 6.2 of the EC3) [11] of the corresponding column, and are summarized in the Table 5.1 of the EC3. For the rolled HEB sections of steel S355 with section flange thickness no >100 mm and section height to width ratio less or equal to 1.2 (up to HEB 360, what applies to all the cases of HEB profiles in this study), the relative initial local bow imperfections (for plastic analysis) are 1/200 and 1/150 (of the column height) for the buckling about the major principal axis and the minor principal axis of HEB cross-section respectively. For elastic analysis, these values would be 1/250 and 1/200 (for buckling about major and minor principal axis respectively).

For this approach, the values of material parameters are considered by their design values.

In case the structural resistance is determined considering above mentioned imperfections and the design values of material, the results are noted with "#EC3" mark.

2.2. Structural resistance based on first-order reliability method (FORM)

The structural reliability is expressed as a function of random load effect E and random resistance R. The safety margin M is then defined as:

$$M = R - E \geq 0 \tag{4}$$

The failure probability P_f is expressed as:

$$P_f = P(R < E) = P(R - E < 0) = P(M < 0) \tag{5}$$

where R and E are statistically independent variables (uncorrelated); both defined by Gauss PDF with the mean values μ_R, μ_E, and the standard deviations σ_R, σ_E respectively. The safety margin M is described by Gauss PDF defined by mean value μ_M and standard deviation σ_M, expressed as:

$$\mu_M = \mu_R - \mu_E \tag{6}$$

$$\sigma_M = \sqrt{{\sigma_R}^2 + {\sigma_E}^2} \tag{7}$$

By the integration of PDF function of random variable M, the probability of $R - E = M < 0$ is then expressed as:

$$P_f = \int_{\infty}^{0} f_M dm = \Phi\left(\frac{0 - \mu_M}{\sigma_M}\right) = \Phi(-\beta) \tag{8}$$

where $\Phi()$ is the normalized cumulative Gauss distribution and the ratio μ_M/σ_M is the reliability index β. Considering the reliability class RC2, which corresponds with the consequence class CC2, and the reference time of 50 years, see Chapter B.3.2(2) of annex B EN 1990 [29] or application [40], the required value of the reliability index for structural members is $\beta_d = 3.8$. The probability of failure is then equal to $P_f = \Phi(-3.8) = 7.2 \cdot 10^{-5}$. In general, the structural reliability can be verified by the reliability index:

$$\beta = \frac{\mu_M}{\sigma_M} \geq \beta_d \tag{9}$$

The probabilistic design condition $P_f < P_{fd}$ (where P_{fd} is the target value of the failure probability [29]) is obtained by the substitution of Eq. (9) into Eq. (8). Eq. (7) might be transformed by the introduction of FORM sensitivity factors α_E, and α_R:

$$\sigma_M = \frac{{\sigma_R}^2 + {\sigma_E}^2}{\sqrt{{\sigma_R}^2 + {\sigma_E}^2}} = \frac{\sigma_R}{\sqrt{{\sigma_R}^2 + {\sigma_E}^2}}\sigma_R + \frac{\sigma_E}{\sqrt{{\sigma_R}^2 + {\sigma_E}^2}}\sigma_E \tag{10}$$

$$\sigma_M = \alpha_R \sigma_R + \alpha_E \sigma_E \tag{11}$$

For common design conditions (Gauss PDF, common values of σ_R and σ_E), it is allowed to use constant values $\alpha_R = 0.8$ and $\alpha_E = 0.7$, as proposed by Chapter C.7(3) of annex C of EN 1990 [29]. This simplification results in $\sigma_M \approx 0.8\,\sigma_R + 0.7\,\sigma_E$. The design condition of reliability is then obtained by substituting Eq. (6) and Eq. (11) into Eq. (9):

$$\mu_E + \alpha_E \beta_d \sigma_E \leq \mu_R - \alpha_R \beta_d \sigma_R \tag{12}$$

The values of the design resistance R_d and the design load E_d are expressed by the right and left sides of Eq. (12) respectively. For $\alpha_R = 0.8$ and $\beta_d = 3.8$, the design resistance R_d is:

$$R_d = \mu_R - 0.8 \cdot 3.8 \cdot \sigma_R \tag{13}$$

The probability, that the structural resistance R is smaller than the design value of the structural resistance R_d is then expressed as:

$$P(R \leq R_d) = \Phi\left(\frac{\mu_R - \alpha_R \beta_d \sigma_R - \mu_R}{\sigma_R}\right) = \Phi(-\alpha_R \beta_d). \tag{14}$$

In this study, the reliability index $\beta = \beta_d = 3.8$ and the FORM sensitivity factor for the structural resistance $\alpha_R = 0.8$ are adopted. Hence, the probability, that the structural resistance R_d calculated by this approach is smaller than the design resistance R is approximately $\Phi(-0.8 \cdot 3.8) = 0.118\%$. This value is approximately applicable as a 0.1% quantile of resistance PDF [41] [42], hence the values of structural resistances discussed in this study based on FORM are determined by the use of Eq. (13). The same approach to determine the structural resistance has been utilized in the previous studies, e.g. [43–45].

3. Erection tolerances of multi-storey steel frames

Statistical values of parameters (initial geometrical imperfections) for the FORM method, might be derived from standard which defines the erection tolerance criteria, EN 1090–2:2018 [38]. Analogically, the values might be obtained from large sample of real construction site measurements, e.g. summarized in a research study by Lindner and Gietzel [46]. Similar values have been adopted by Shayan et al. [4]. The values in this study have been derived from the erection tolerance standard, as both approaches would result in similar data.

3.1. Eurocode standard requirements – Tolerance criteria

The erection tolerances for multi-storey steel buildings are considered in accordance with the Table B.18 of the Annex B of standard EN 1090–2:2018 [38]. Two classes of functional tolerances are shown. Class 1 should be applied unless otherwise specified by the execution specification, where consideration of Class 2 (stricter) can be necessary if a glazed façade is to be fitted, as mentioned in the chapter 11.3.2 of EN

1090–2:2018 [38]. In this study, functional tolerances of the Class 1 are considered for all the manufacturer and erection tolerances.

The permitted deviation Δ_i for the location of the storey level located i levels above the base relative to the position of that base, also noted as cumulative tolerance, is expressed as:

$$|\Delta_i| \le \frac{\sum_{j=1}^{i} h_j}{300\sqrt{i}} \tag{15}$$

where h_j is the height of the j-th storey.

Functional tolerance for the criterion of maximal column inclination between two adjacent storey levels i-1 and i marked as $\Delta_{dif,i,i\text{-}1}$, also noted as a storey sway is:

$$\left|\Delta_{dif,i,i-1}\right| \le \frac{h_i}{300} \tag{16}$$

where h_i is the column height (storey height) between these two adjacent storeys.

Functional tolerance for the straightness of a continuous column between adjacent storey levels, also noted as bow imperfection of the column, marked as LI_k (local imperfection) is limited to the value:

$$|LI_k| \le \frac{h_k}{1000} \tag{17}$$

where h_k is the height of the column k.

Graphical depictions of these three criterions are in the **Fig. 1**, for the m-storey structure.

3.2. Stochastic values of the erection tolerances, methods, correlations

In case the frame geometry is to be considered stochastically for subsequent numerical analysis, so called 2 sigma rule might be used in order to achieve maximum 5% of random realizations not fulfilling the considered tolerance criterion.

Local imperfection model, described in Chapter 3.2.1, is considered in all FORM method calculations. However, when analyzing the geometrical deviation of each storey, two criteria come into analysis. Stochastic values can be determined through two different approaches, #RSS and #RSP, as outlined in Chapters 3.2.2 and 3.2.3, and also [39].

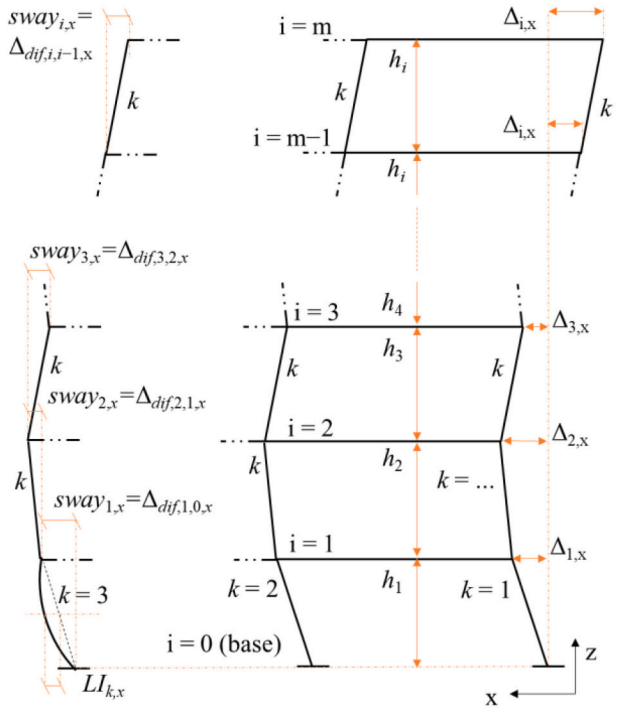

Fig. 1. Tolerance criterions of steel frame structure for the x direction of GCS

3.2.1. Local imperfections

For simplification, the random local imperfection LI, of all the columns of certain floor is considered as the same for the corresponding direction (two horizontal global directions are considered, x and y) – e.g., in case of n-storey frame, there are all together 2n random input parameters noted as LI_{x1}, … LI_{xn} and LI_{y1}, … LI_{yn}, where LI_{xn} is the local imperfection (bow imperfection) for all the columns of n-th floor in the global x direction. The statistical parameters are based on the tolerance criterion, Eq. (17), and as described in the chapter 3.2, the mean is considered as 0, with the standard deviation as 1/2000 of the column height, considered as the bow imperfection in the mid-height of the column. The shape of the bow imperfection is considered as half wave of a sinusoid. Any additional local imperfection (e.g. in a shape of the whole sinusoid wave, or 3 sinus half-waves), as was discussed e.g. by Shayan et al. [4] have been neglected in order not to implement too many random input parameters.

3.2.2. Random storey sway (#RSS) method

The first approach is to consider the random input of sways for each storey (noted as $sway_{i,x}$ in the **Fig. 1**, or further also in short variant $sw_{i,x}$). Based on Eq. (16), the mean value of 0, and standard deviation of 1/600 rad (based on 2 sigma rule) are considered. This approach is further noted as "random storey sways" method (approach #RSS). The deviations of two adjacent storeys are limited by these sway values and the fact, that the geometry of each storey is bonded to the position of the storey below, hence the location of each storey relative to the base (the second criterion to be verified) is already partially indirectly incorporated in the logic of what is considered as random parameter for input.

For this method, the subsequent verifications of the random realizations number which violate the criteria of storey deviation relative to the position of the base, Eq. (15), is suitable to be conducted. Hence, whether approximately 5% of random realizations would violate criterion for the corresponding storey, verified for each storey of the structure separately. It has been statistically verified, that the number of random realizations which would violate the criteria for the storey positions relative to the base is 4.56% for the 1st storey, around 4% for the 15th storey, and 3.73% for the 23rd storey. This decrease appears to be approximately linear, in average − 0.0375% per storey.

Overall, the #RSS approach might be used without any additional modification for smaller amount of floors. For larger number of storeys, it is questionable, whether the number of realizations which violate the cumulative tolerances (Eq. (15)) for the uppermost floors is not too small, as the value is not so close to the 5% threshold.

3.2.3. Random storey position (#RSP) method

In this approach, the stochastic input values are the storey deviations relative to the position of the base (noted as $\Delta_{i,x}$ in the **Fig. 1**), with mean values of 0 mm for each storey. The standard deviations are derived for each storey based on the Eq. (15), hence larger values with increasing level of the corresponding storey (using 2 sigma rule).

In this case, certain correlations (positive) between these input parameters need to be introduced, mainly for multiple storey structures, as otherwise this approach would lack any relation between two adjacent storeys, resulting in too many realizations violating the criteria of storey sway (Eq. 16). These input storey deviations relative to the base are mutually correlated through the Gaussian correlation function (Eq. 18), which represents a 1D random field with correlation length L_{cor} [m] and was used also in [41,42]:

$$\rho_{jh} = p \cdot e^{-\left(\zeta_{jh}/L_{cor}\right)^2} \tag{18}$$

where ρ_{jh} is the member of the correlation matrix, p is the multiplication

factor to ensure the matrix is positive definite (applicable mainly for larger matrixes, considered as 0.99, except for diagonal matrix members which are exactly 1.0), ζ_{jh} is the vertical distance between two points (two floors).

The correlation length L_{cor} might be expressed relatively as ω ratio:

$$\omega(m) = \frac{L_{cor}}{m\,h} \tag{19}$$

where m is the total number of floors, each of height h. As far as the vertical distance of two floors ζ_{jh} might be expressed as natural multiplication $n{\cdot}h$ of the storey height h, the Eq. 18 might be expressed as:

$$\rho_{jh} = p{\cdot}e^{-\left(\frac{n}{\omega(m)\cdot m}\right)^2} \tag{20}$$

where n is the relative distance between two floors (e.g. $n = 1$ for the distance between the 1st floor and the 2nd floor).

It is suitable to use the smallest possible value of the correlation length L_{cor}, the optimal correlation length, which would secure, that the number of random realizations which violate the sway tolerances (Eq. 16) are below 5% for each storey of the m-storey structure.

In order to achieve this, the L_{cor} is derived from the relative ω ratio in dependence on the number of storeys m, summarized in the Table 1.

These ω ratio values have been numerically determined in previous study [39] considering numerous random generations of Δ_i input values of a m-storey structures ($m = 2$ to 24). An algorithm to found optimal ω ratio for each m-storey structure has been used, where the ratio of random realizations violating the sway tolerance (Eq. 16) of that m^{th} storey is equal to 5% ± 0.2%. This approach of #RSP might be also used to verify the already utilized #RSS in case of 3-storey frame structure analysis [47].

4. Numerical finite element models (FEM)

4.1. Input values of statistical parameters for FORM method

To conduct the first-order reliability analysis (FORM) utilizing GMNIA (geometrically and materially nonlinear imperfect analyses), statistical data on input parameters (material, geometric and imperfection) is required.

ANSYS Classic technology (v.19) [36] with APDL (ANSYS parametric design language) scripts have been used to create a parametrized numerical finite element models of various steel frame structures. The number of random input parameters is different for each frame, and depends on the number of floors.

Table 1
Summary of the optimal correlation values expressed by the relative ratio ω.

m storey structure	$\omega(m)$ [−]
2	0.8333
3	0.7259
4	0.6500
5	0.6098
6	0.5744
7	0.5416
8	0.5128
9	0.4872
10	0.4764
11	0.4513
12	0.4444
13	0.4376
14	0.4222
15	0.4133
16	0.4097
17	0.3967
18	0.3942
19	0.3953
20	0.3889
21	0.3869
22	0.3838
23	0.3845
24	0.3815

Local imperfections are described in the chapter 3.2.1.

Furthermore, for each storey, there are random global geometrical imperfections defined for both global directions, x and y. The logic of this definition depends on the used approach, #RSS or #RSP, as described in the chapters 3.2.2 and 3.2.3 respectively. In both cases, there are additional 2n random parameters for the n-storey frame.

Material of the steel (S355) is considered as linear elastic, ideal plastic, with the mean value of E modulus = 210 GPa, and the standard deviation of 10.5 GPa. The mean value of the yield stress f_y is considered as 393.8 MPa and the standard deviation as 22 MPa [47]. Bilinear material model with isotropic hardening and von Mises yield criterion has been considered (otherwise kinematic hardening is commonly used if the unloading of the steel structures is being modelled [36]). Tangent modulus (the slope of stress-strain diagram after the yield stress) was considered always as 5% of the Elastic modulus, E value. This simplification has been considered, as the point, when plastic strains occurs in certain beam element (column), is already very close to the global ultimate resistance of the steel frame. Poisson ratio has been considered with the constant value of $\nu = 0.3$, as discussed in the stochastic sensitivity study by Kala [45].

Normal Gauss distributions are considered for all the stochastic input parameters. The probability density function (PDF) might be considered as Gaussian for geometrical imperfections, as this assumption is commonly used in conventional stochastic models [3,4,47]. Concerning material parameters, according to study by Sakai et al. [48], the tensile properties of steel materials, as yield stress, is governed by normal distributions, while log-normal distributions also might be used. Normal distribution was also suggested by Sekulski for the yield stress of structural steel [49], and considered also for yield stress of steel reinforcement bars by Stefano et al. [50]. On the other hand, log-normal distributions were used for yield stress and Elastic modulus during the analysis of offshore wind turbines by Muskulus et al. [51]. For three different stainless steel grades, normal distributions are suggested for Elastic modulus and log-normal distribution for 0.2% proof stress conventionally adopted as the equivalent yield stress [52]. Adopting a log-normal distribution for certain parameters has the advantage, that no negative values can be randomly generated, as also noted by EN 1990 [29], what is not case of material parameter values in this study, hence normal Gaussian distributions were preferred [48].

In summary, for n-storey frame, there are together 4n + 2 random input parameters: 2 material variables, 2n parameters for the local bow imperfection amplitude of the columns, and 2n global imperfections for stories (in global x and y directions).

4.2. Geometries of the models, boundary conditions, loading

In all the cases, 1D structural beam finite elements are utilized for numerical model of the steel frames. Structural spans, cross-sections and dimensions of the members are described in the subsequent chapters. For all the frame models, all 6 Degrees of Freedom (DoF) are constrained at the ground level of coordinate z = 0. All the columns are oriented in a way, that the “less rigid cross-section axis” is parallel with x-axis of the global coordinate system (GCS). No effects of beam-to-column joint stiffness or the floor slab stiffness have been considered. For simplification, ideally rigid connections are assumed in the beam connections. Each column is being modelled by 10 finite elements, and the horizontal beams are discretized into 5 finite elements. This mesh density has been selected based on the results of short mesh size study, where various mesh sizes of the frame geometry #3 × 3 × 8 (further explained in this chapter) have been analysed. Ultimate resistance $N_{u,EN}$ (as further explained in the chapter 5 and 5.2) has been monitored, and the results are depicted in the Table 2. The considered mesh size appears to be good

Table 2
Mesh size study.

Case of frame geometry #3 × 3 × 8	Mesh – number of elements per each		$N_{u,EN}$ [kN]	$N_{u,EN}$ difference with case D [%]	Analysis time using 2 CPUs [seconds]	
	Column	Horizontal beam			Total time summed for all threads	Elapsed time (physical)
A	5	2	51,291	2.0	105	60
B	10	5	50,694	0.8	204	110
C	20	10	50,428	0.3	367	195
D	30	15	50,291	0.0	573	309

compromise between the accuracy and time of the calculation. The comparison of analysis time is done on Intel Xeon E5 1620 0 (Sandy Bridge-EP) 3.6 GHz, using 2 CPUs from the total number of 4 CPU's.

Type of the finite elements is BEAM188 – based on Timoshenko beam theory which includes shear-deformation effects. BEAM188 was considered with 6 degrees of freedom (DoF) at each node: translations in the x, y, z directions and rotations about the x, y, and z directions. The 6th DoF variant of BEAM188 considers unrestrained warping. The option to include the 7th DoF per node (including warping) has not been used. For some frame cases, diagonal bracings are also considered. If applicable, each bracing is modelled by one single LINK180 finite element, with tension-only formulation. Hence, no initial geometrical imperfections of the braces were considered. Link element has 3 DoF at each node: translations in the nodal x, y, z axis. There was no initial prestress applied in these tension-only braces. By these assumptions, state of bracing just before stretching and introduction of the prestress is being modelled.

The geometry of the simplest frame noted as #1 × 1 × 1 (numbers indicates span numbers in x, y and z directions) is analysed in this study is depicted in the Fig. 2. All the columns are HEB 240, beams in x direction are IPE 270 and in y direction IPE 300. No diagonal bracings. Loading of the frame is considered in nodal points of column-beam intersections.

The geometry of frame noted as #1 × 1 × 2 is depicted in the Fig. 3. The first floor is practically the same as in case of the #1 × 1 × 1. All the columns of the 2nd floor are HEB 200, and the beams are of profile IPE 220 for the x direction and IPE 240 in the y direction. Loading applied at each floor in beam-column intersections.

The Fig. 4 depicts frame noted as #1 × 1 × 3. In basic, this is case #1 × 1 × 2 with the columns and beams of the 3rd floor the same as in the 2nd floor. Loading applied at each floor in beam-column intersections.

Cases #1 × 1 × 4_LF and #1 × 1 × 4_AF depicted in the Fig. 5 have HEB 220 as columns of the 1st floor, and HEB 200 for the 2nd – 4th floors. Beams in x and y directions are of the same cross-section for each floor: for the 1st, IPE 330 and for the 2nd – 4th floors IPE 300. These case differ in the loading, which is either applied in the beam-column intersections of the last 4th floor only, or at each floor, hence the

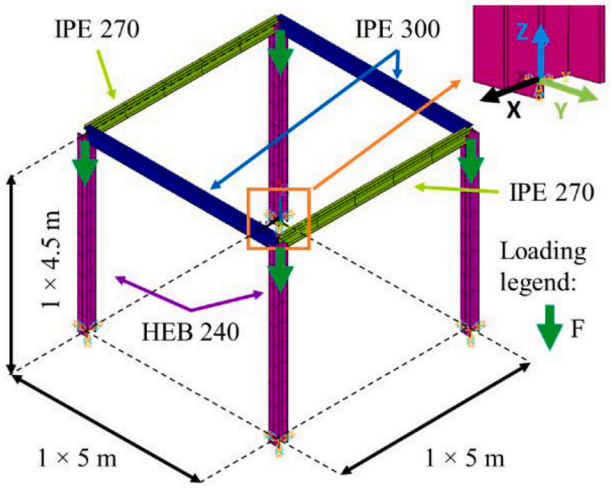

Fig. 2. Geometry of the steel frame #1 × 1 × 1_AF

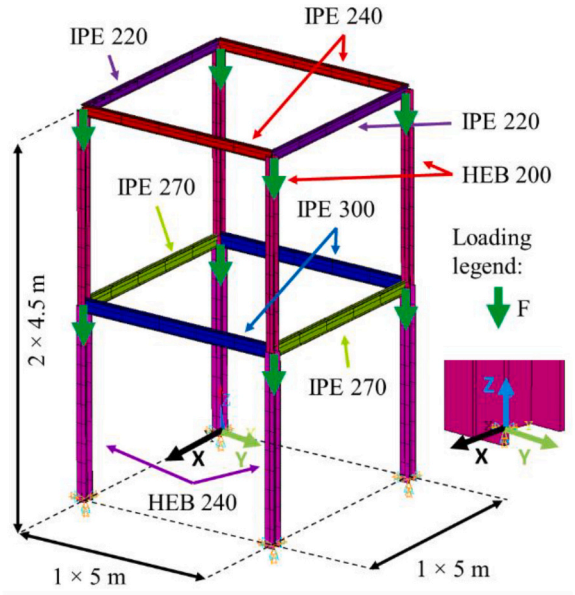

Fig. 3. Geometry of the steel frame #1 × 1 × 2_AF

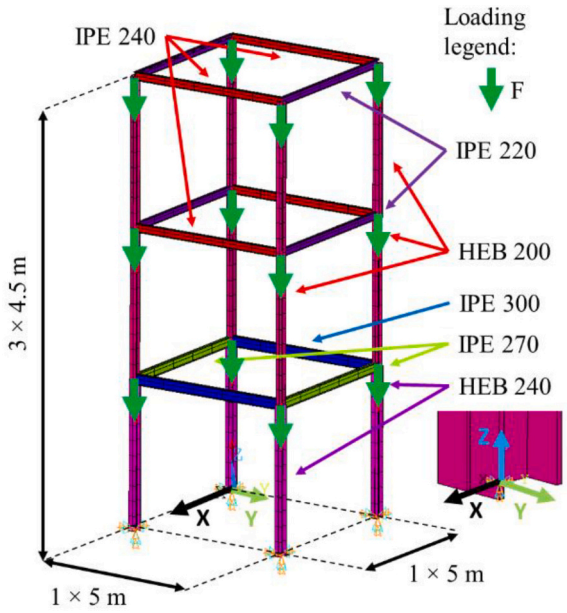

Fig. 4. Geometry of the steel frame #1 × 1 × 3_AF

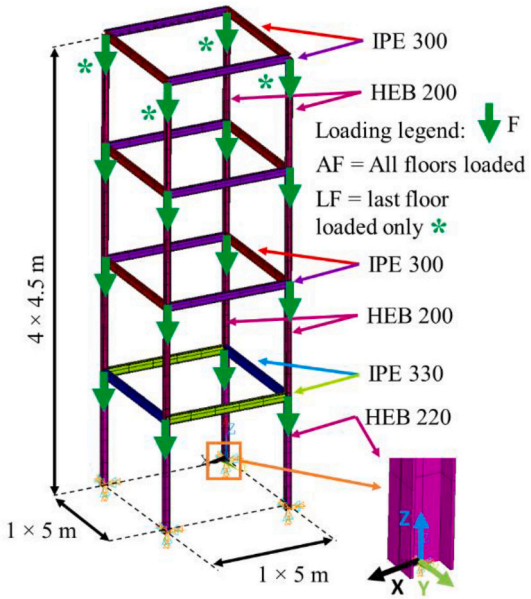

Fig. 5. Geometry of the steel frame #1 × 1 × 4_AF and #1 × 1 × 4_LF

abbreviations of "LF" and "AF" for the meaning "last floor" and "all floors" respectively.

Geometry of the case #3 × 3 × 8 is depicted in the Fig. 6. The cross-sections of the columns are in accordance with the planar views and depends on the floor number. Horizontal beams are the same through the whole height, IPE 330 in both directions. Diagonal bracings are located at all four facades sides, in the middle segments. These tension-only elements are defined by the cross-section areas, which matches the circles of the provided diameters: Ø34 mm, Ø26 mm and Ø18 mm (Fig. 6). Loading is applied at each floor in beam-column intersections. This presented case #3 × 3 × 8 is considered as rather realistic geometry of a structure.

On the other hand, to test what the differences of the results might be no matter whether the geometry is feasible for the real-world structure, hence to test some theoretical limits, the geometry of the case #1 × 1 × 24 has been considered, and is depicted in the Fig. 7. This rather unreal geometry frame has one span in each horizontal directions, and 24 floors, each of 3.6 m height. The cross-sections are the same for each floor, and described in the Fig. 7.

Note: the HEB and IPE cross-section geometries have been obtained from the corresponding web tables of staticstools.eu [53]. The radius of root fillet r [53] (the roundings between the section web and flange) have been neglected (hence only negligibly smaller section area and second moment of areas are considered).

5. FEM simulations

Geometrically and materially nonlinear imperfect analyses (GMNIA) have been conducted in order to determine the structural resistance. In the first step of the geometrically nonlinear analysis, the self-weight load is applied by gravitational acceleration of 9.81 m/s2 (steel material density of 7850 kg/m3 is considered as deterministic value for all the cases). In the second and all the subsequent steps of loading process, the

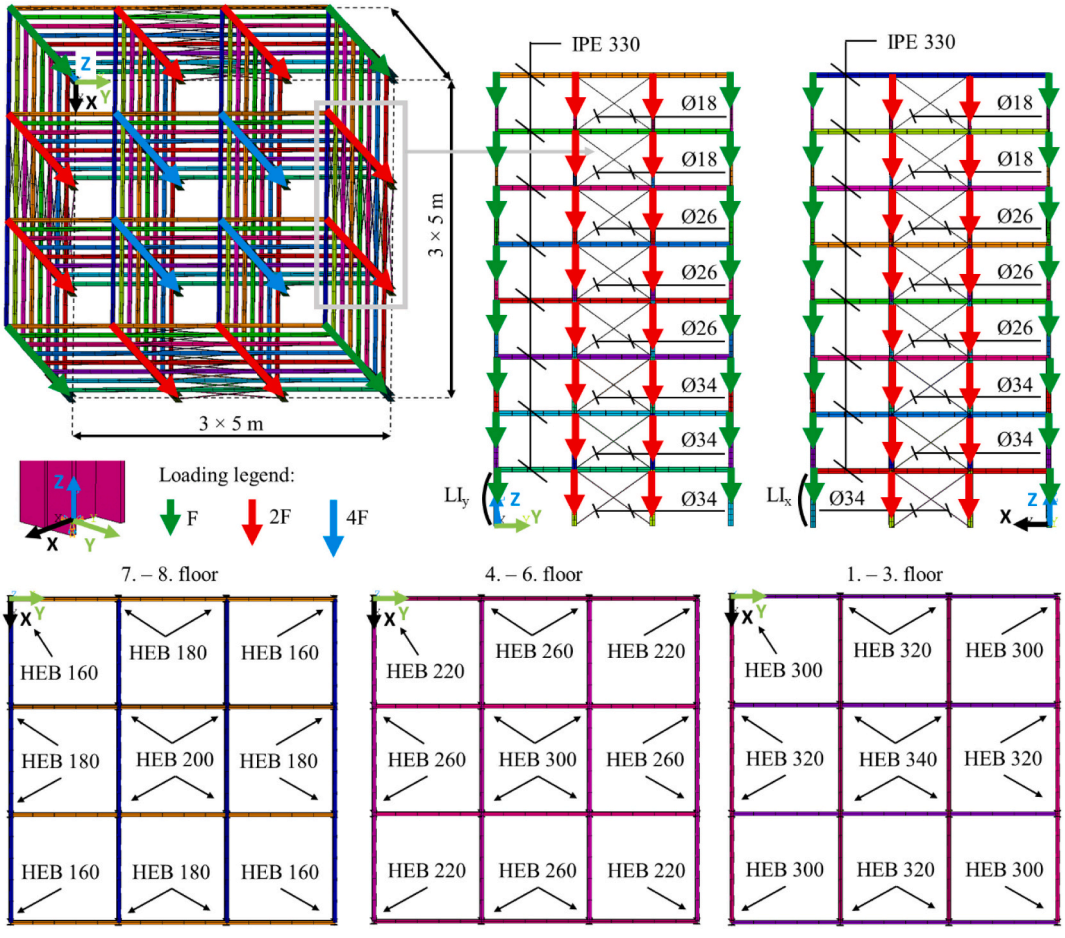

Fig. 6. Geometry of the steel frame #3 × 3 × 8_AF

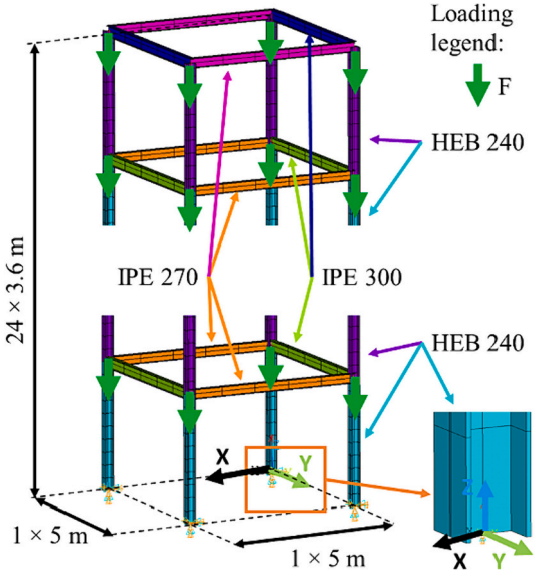

Fig. 7. Geometry of the steel frame #1 × 1 × 24_AF

structural nodal forces are added in corresponding positions, depending on the analysed frame (see chapter 4.2, Fig. 2 – Fig. 7). The sum of vertical reaction R_z is being monitored during this process, and the ultimate resistance N_u is determined as the reaction resultant R_z of the last converged step of the analysis (default convergence criteria of ANSYS software).

5.1. The structural resistance estimation

The article examines structural resistance using the FEM model, wherein resistance is estimated through the step-by-step method of increasing force load. Generally, resistance can be estimated by two fundamental approaches: force loading and deformation loading.

Force loading yields more realistic deformations, crucial for analyzing the impact of initial imperfections. However, the downside is that increasing force may lead to convergence issues near the curve's peak, which can be effectively addressed by numerically setting up the computation.

The disadvantages of applying deformation loads, however, are more pronounced. Most frame geometries are loaded on each floor, complicating the application of multiple interdependent deformation loads across all levels and potentially causing unnatural structural deformations. The advantage of deformation loading is that it allows for easier attainment of the peak of the load vs. deformation curve.

In case studies comparing force and deformation loading, it was necessary to select a load action that would prevent unnatural structural deformations. For this reason, deformation loading was applied only to the top floor, utilizing a uniform prescribed vertical displacement, while gravitational loading was neglected. Two types of frames were analysed, as seen in Fig. 8 and Fig. 9.

Analysis of frame geometry, subjected to both force and prescribed displacement, revealed negligible differences in ultimate resistance, as depicted in Fig. 8. Although convergence issues from force loading may occur near the peak of the load-displacement curve, they can be effectively resolved by using a very small load step close to the N_u point.

Fig. 9 illustrates the calculation of $N_{u,EN}$ (N_u under EC3 assumptions – see chapter 5.2) using force loading (represented by the blue curve), where the peak of the curve is reached with the aid of deformation loading (represented by the orange curve). After the last force convergence point, the analysis continued with deformation loading. The estimated ultimate resistances, $N_{u,EN}$, are 8.9192 and 8.9297, with a difference of 0.12%, as seen in the Fig. 9.

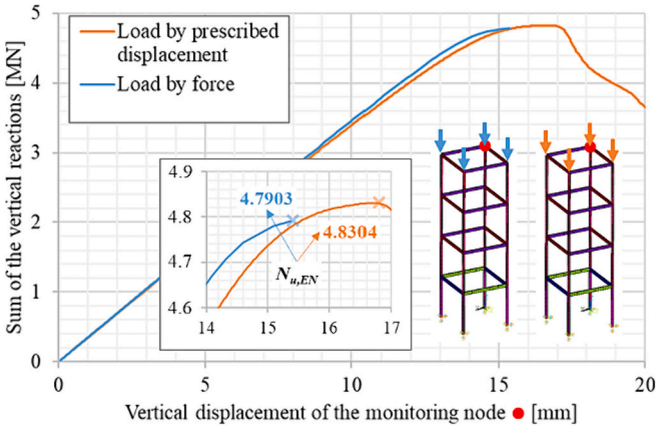

Fig. 8. Case study of the model #1 × 1 × 4_LF performance when loaded by force and prescribed displacement

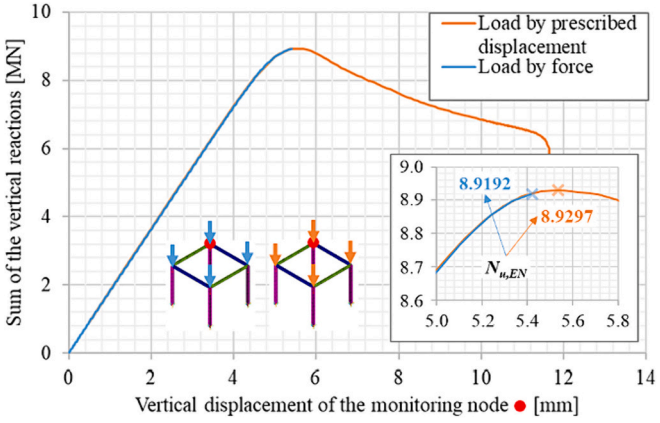

Fig. 9. Case study of the model #1 × 1 × 1 performance when loaded by force and prescribed displacement

Although it would be ideal to estimate the top point using subsequent deformation loading for all frames and all loading conditions, this approach can be complex in cases where the frame is loaded on every floor. In selected cases, we verified that a very similar accuracy in estimating $N_{u,EN}$, as illustrated in Fig. 9, was achieved in other selected simulations as well. The minor relative differences observed in these cases (0.8% and 0.1%) are deemed negligible. Thus, it can be summarized that the estimation of structural resistance using force loading can be considered sufficiently accurate.

For the solution, the full Newton-Rapson equation formulation was used, using standard convergence criteria according to M-F internal forces [36]. The initial increment was chosen with a size corresponding to one tenth of the total applied load, which is approximately twice the mean value of N_u. An automatic algorithm was used for subsequent load increment sizes, which decides the increment according to the speed of convergence of the previous step. In case no solution is found, the increment is reduced. Decreasing the increment continues until the minimum step is reached. The minimum step was applied in a size corresponding to 0.05% of the applied load. This defines the numerical accuracy of achieving the bearing capacity.

5.2. #EC3 approach

For each considered frame type (chapter 4.2), only one numerical GMNIA analysis is conducted in order to determine the structural resistance N_u in accordance with the EC3 assumptions. This value is considered as the design ultimate resistance, noted as $N_{u,EN}$, as the

design values of input parameters have been used.

5.3. #FORM approach

The statistical input data are discussed is the chapter 4.1. Two approaches, #RSS and #RSP, how to consider the input of global imperfection are described in the chapters 3.2.1 and 3.2.2 respectively. In both approaches, the Advanced Latin Hypercube Sampling (ALHS) method has been used to generate the random realizations of the input parameters. In this method, the correlation errors are minimized by the stochastic evolution strategies [54]. The representation of the specified input distributions and the input correlations is also very accurate when the standard Latin Hypercube Sampling (LHS) method [55] is used, where a method to minimize the undesired correlations is implemented, Iman and Conover [56]. ALHS was preferred, as it is recommended for not so large number of input parameters [57]. The software OptiSLang [57] has been used to manage the ANSYS solver [36]. 2000 random realization have been numerically analysed for each case of steel frame geometry.

5.3.1. Statistical verification

In order to check the statistical validity of the results, the Gaussian distribution of the results was verified utilizing so-called "goodness-of-fit" tests [58]. Two distribution tests have been verified: Anderson-Darling [59] and Kolmogorov-Smirnov [60,61]. The purpose of these tests is to confirm, that a certain probability distribution (e.g., normal distribution) might be feasibly utilized for the description of a population sample. It was revealed, that the hypothesis of Gauss distribution of the results (ultimate resistance N_u) was not rejected (1% significance level) based on the results of both tests for all the analysed cases. Therefore, the conclusion of these test is, that ultimate resistances N_u based on the finite element simulations might be considered as normally distributed. Hence for each set of 2000 analyses, the 0.1% quantile of the structural resistances N_u is considered as the design ultimate resistance based on FORM method, noted as $N_{u,FORM}$ (determined by the Eq. 13).

6. Results

6.1. Ultimate resistances

The results of all the analysed cases are summarized in the Table 3. Case names are in the first column of the table. The geometry of frames for these cases is closely described in the chapter 4.2. In short, the "x × y × z" stands for the number of spans in two horizontal (x,y) and vertical direction (z – number of floors). "AF" or "LF" stands for "all floors" or "last floor" respectively, and indicates the applied loading (see the chapter 4.2). The #RSS and #RSP stands for the method of applied imperfections, the "random storey sway" or "random storey position" – as described in the chapter 3.2.

The estimations of the slenderness values $\bar{\lambda}_1$; $\bar{\lambda}_2$ for the columns of the first and (if applicable) the second floor respectively are summarized in the second column of the table Table 3. The relative slenderness values are determined in dependence on the cross-section area A, and the yield stress f_y (355 MPa) as:

$$\bar{\lambda}_i = \sqrt{\frac{A \cdot f_y}{N_{cr,i}}} \tag{21}$$

where $N_{cr,i}$ is the critical Euler force, which was derived from the results of the linear stability analysis (eigenvalue buckling), always using the first critical eigenvalue – factor α_1, and normal force N_i of the column from the corresponding i-th floor taken from the initial stress calculation, which is prior to the eigenvalue buckling analysis:

$$N_{cr,i} = \alpha_1 N_i \tag{22}$$

The values are determined only for the columns of the first and second floor, and only for those model cases, where the normal force N_i of all the columns from the corresponding floor are the same. For the more complex geometry of the case #3 × 3 × 8_AF, the relative slenderness values have not been estimated.

In the third column of the Table 3, which is applicable only for the cases calculated by the #RSP method, the used correlation length L_{cor} is provided (see chapter 3.2.3). Subsequent columns denote the mean value of ultimate resistance, $N_{u,mean}$, standard deviation $N_{u,\sigma}$, coefficient of variation $N_{u,CoV}$, and ultimate resistance determined by the FORM method, $N_{u,FORM}$. The last column summarizes ultimate resistance $N_{u,EN}$, based on the EC3 assumptions. The values for the cases of the #RSP approach are marked by asterisk "*", as formally the EC3 approach considers the definition of the sway for the whole structure, hence the value is the same as the corresponding case of #RSS method. Results of the selected cases are graphically depicted in the **Fig. 10**, where values based on FORM method and the EC3 approach are compared.

Note: the resistance of the case #1 × 1 × 24_AF_RSS is larger than in the other cases due to smaller height of the floor (**Figs. 2–5** and **Fig. 7**), rather more stiff cross-section of the columns through the whole height, and compared to the case #1 × 1 × 1 also smaller angle ϕ for the structure sway applied for the EC3 calculation (as for smaller structure, the angle tends to be larger due to α_h coefficient – Eq. 2).

The structural resistance determined by the EC3 approach is larger for majority of the analysed cases, with exception of the #3 × 3 × 8 and #1 × 1 × 24 (Table 3). For the analysed cases, the ultimate resistance determined in accordance with the #RSP approach results only in negligibly different values then if #RSS approach is considered – see also graphical depiction in the **Fig. 11**. The only exception is the case #1 × 1 × 24, where there is circa 12% difference in the ultimate resistances by #RSS and #RSP approach. However, for the more realistic geometry of the frame structure, e.g. case #3 × 3 × 8, the difference is rather negligible, if the properly considered correlation length is used. As shown in #1 × 1 × 4_LF, the un properly considered correlation length might result in rather large deviation from the result by the #RSS

Table 3
Summary of analysed cases.

Case	Slenderness $\bar{\lambda}_1$; $\bar{\lambda}_2$	L_{cor} (RSP) [m]	$N_{u,mean}$ [kN]	$N_{u,\sigma}$ [kN]	$N_{u,CoV}$ [%]	$N_{u,FORM}$ [kN]	$N_{u,EN}$ [kN]
#1 × 1 × 1_AF_RSS	1.04	–	11,366	1021	8.99	8261	8919
#1 × 1 × 2_AF_RSS	1.13; 1.37	–	10,483	711	6.78	8321	8887
#1 × 1 × 3_AF_RSS	1.28; 1.35	–	8311	674	8.10	6264	7271
#1 × 1 × 4_AF_RSS	1.19; 1.27	–	8110	589	7.26	6320	6796
#1 × 1 × 4_AF_RSP	1.19; 1.27	11.70	8182	565	6.90	6465	6796 *
#1 × 1 × 4_LF_RSS	1.45; 1.34	–	5636	336	5.96	4616	4830
#1 × 1 × 4_LF_RSP	1.45; 1.34	0.00	5286	430	8.13	3980	4830 *
#1 × 1 × 4_LF_RSP	1.45; 1.34	11.70	5628	351	6.24	4561	4830 *
#1 × 1 × 4_LF_RSP	1.45; 1.34	999.00	5830	311	5.34	4883	4830 *
#3 × 3 × 8_AF_RSS	–	–	58,551	2441	4.17	51,130	50,694
#3 × 3 × 8_AF_RSP	–	14.77	58,534	2446	4.18	51,098	50,694 *
#1 × 1 × 24_AF_RSS	1.05; 1.07	–	11,765	689	5.86	9669	9169
#1 × 1 × 24_AF_RSP	1.05; 1.07	32.96	12,846	644	5.01	10,888	9169 *

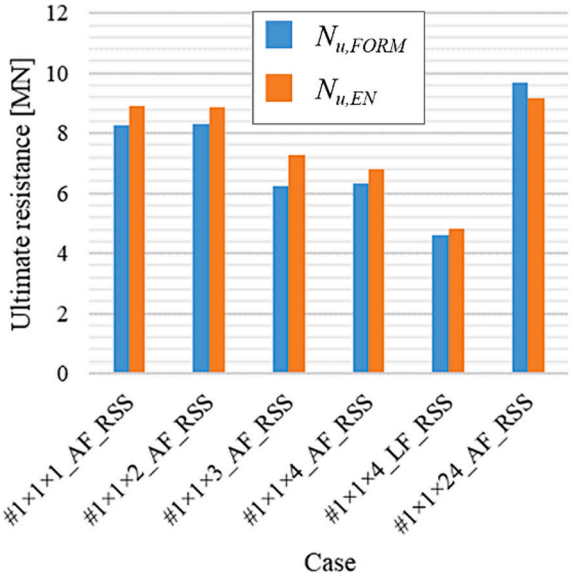

Fig. 10. Comparison of the ultimate resistances between EC3 and FORM approaches

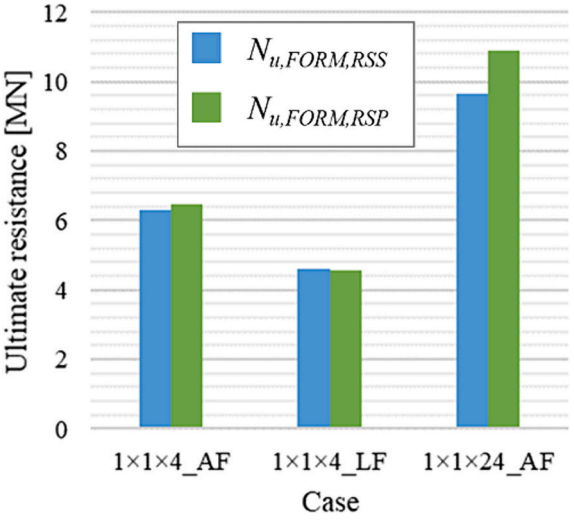

Fig. 11. Comparison of the ultimate resistances between #RSS and #RSP method of the FORM approach

approach.

6.2. Failure modes

The overall deformations of each single random realization differs, as it predominantly follows the pattern of the random initial imperfection, most significantly sway imperfections of the floors. An example of the displacements in the global y direction of the frame #3 × 3 × 8 (more precisely the case with sway in accordance with EC3) is depicted in the Fig. 12. The inclination of the whole frame is in the direction of the applied geometrical imperfection. Just before the ultimate resistance has been reached, the plastic strains began to appear, as in the example of frame #1 × 1 × 1 depicted in the Fig. 13. Note: equivalent Von Mises strains are considered.

6.3. Correlations

The examples of correlation matrixes (linear, Pearson) for the model

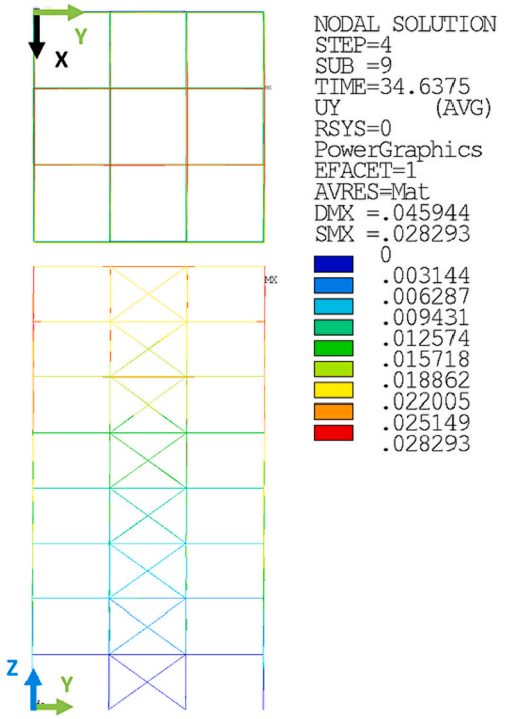

Fig. 12. Example of the failure mode – displacements in the global y direction for the frame #3 × 3 × 8_AF

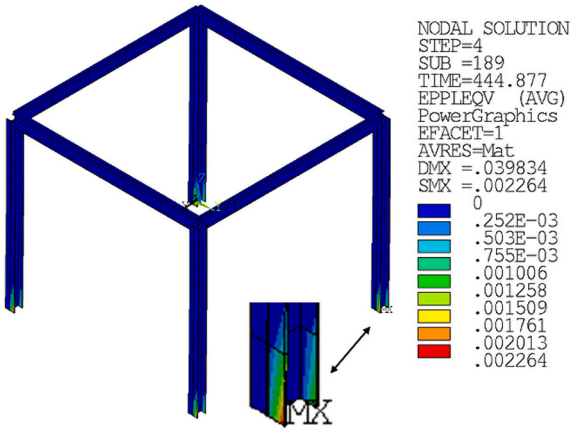

Fig. 13. Example of the plastic strains for the frame #1 × 1 × 1_AF one step before the failure

case #1 × 1 × 4_LF_RSP (for correlation length of 11.7 m) are depicted considering the absolute values of the parameters in the Fig. 14. Analogically, for the case #1 × 1 × 4_LF_RSS, the correlations are in the Fig. 15 and Fig. 16, in absolute values and respecting the signs respectively.

The variables in matrixes are considered in the absolute value in order to capture the correlations between the imperfect parameters (either sway or cumulative tolerances) and the output ultimate resistance N_u (Fig. 14, Fig. 15). A correlation matrix with parameter values respecting the signs for the case #1 × 1 × 4_LF_RSS is depicted in the Fig. 16, as the correlations between the sway inputs and the achieved cumulative deviations will be further discussed. It is evident there are practically 0 correlations between the ultimate resistance and the sway imperfection in the matrix where the signs are being respected (Fig. 16).

Not all the input parameters are plotted in these matrixes, as the local imperfections of columns $LI_{x1} - LI_{x4}$ and $LI_{y1}, - LI_{y4}$, because the matrix

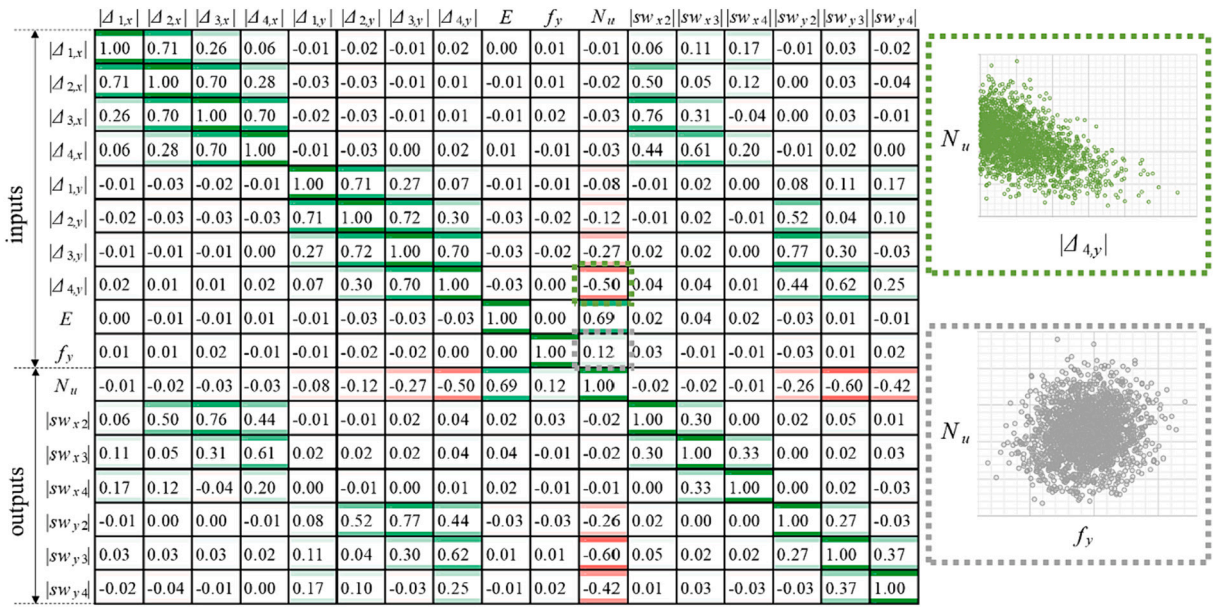

	$\lvert\Delta_{1,x}\rvert$	$\lvert\Delta_{2,x}\rvert$	$\lvert\Delta_{3,x}\rvert$	$\lvert\Delta_{4,x}\rvert$	$\lvert\Delta_{1,y}\rvert$	$\lvert\Delta_{2,y}\rvert$	$\lvert\Delta_{3,y}\rvert$	$\lvert\Delta_{4,y}\rvert$	E	f_y	N_u	$\lvert sw_{x2}\rvert$	$\lvert sw_{x3}\rvert$	$\lvert sw_{x4}\rvert$	$\lvert sw_{y2}\rvert$	$\lvert sw_{y3}\rvert$	$\lvert sw_{y4}\rvert$
$\lvert\Delta_{1,x}\rvert$	1.00	0.71	0.26	0.06	-0.01	-0.02	-0.01	0.02	0.00	0.01	-0.01	0.06	0.11	0.17	-0.01	0.03	-0.02
$\lvert\Delta_{2,x}\rvert$	0.71	1.00	0.70	0.28	-0.03	-0.03	-0.01	0.01	-0.01	0.01	-0.02	0.50	0.05	0.12	0.00	0.03	-0.04
$\lvert\Delta_{3,x}\rvert$	0.26	0.70	1.00	0.70	-0.02	-0.03	-0.01	0.01	-0.01	0.02	-0.03	0.76	0.31	-0.04	0.00	0.03	-0.01
$\lvert\Delta_{4,x}\rvert$	0.06	0.28	0.70	1.00	-0.01	-0.03	0.00	0.02	0.01	-0.01	-0.03	0.44	0.61	0.20	-0.01	0.02	0.00
$\lvert\Delta_{1,y}\rvert$	-0.01	-0.03	-0.02	-0.01	1.00	0.71	0.27	0.07	-0.01	-0.01	-0.08	-0.01	0.02	0.00	0.08	0.11	0.17
$\lvert\Delta_{2,y}\rvert$	-0.02	-0.03	-0.03	-0.03	0.71	1.00	0.72	0.30	-0.03	-0.02	-0.12	-0.01	0.02	-0.01	0.52	0.04	0.10
$\lvert\Delta_{3,y}\rvert$	-0.01	-0.01	-0.01	0.00	0.27	0.72	1.00	0.70	-0.03	-0.02	-0.27	0.02	0.02	0.00	0.77	0.30	-0.03
$\lvert\Delta_{4,y}\rvert$	0.02	0.01	0.01	0.02	0.07	0.30	0.70	1.00	-0.03	0.00	-0.50	0.04	0.04	0.01	0.44	0.62	0.25
E	0.00	-0.01	-0.01	0.01	-0.01	-0.03	-0.03	-0.03	1.00	0.00	0.69	0.02	0.04	0.02	-0.03	0.01	-0.01
f_y	0.01	0.01	0.02	-0.01	-0.01	-0.02	-0.02	0.00	0.00	1.00	0.12	0.03	-0.01	-0.01	-0.03	0.01	0.02
N_u	-0.01	-0.02	-0.03	-0.03	-0.08	-0.12	-0.27	-0.50	0.69	0.12	1.00	-0.02	-0.02	-0.01	-0.26	-0.60	-0.42
$\lvert sw_{x2}\rvert$	0.06	0.50	0.76	0.44	-0.01	-0.01	0.02	0.04	0.02	0.03	-0.02	1.00	0.30	0.00	0.02	0.05	0.01
$\lvert sw_{x3}\rvert$	0.11	0.05	0.31	0.61	0.02	0.02	0.02	0.04	0.04	-0.01	-0.02	0.30	1.00	0.33	0.00	0.02	0.03
$\lvert sw_{x4}\rvert$	0.17	0.12	-0.04	0.20	0.00	-0.01	0.00	0.01	0.02	-0.01	-0.01	0.00	0.33	1.00	0.00	0.02	-0.03
$\lvert sw_{y2}\rvert$	-0.01	0.00	0.00	-0.01	0.08	0.52	0.77	0.44	-0.03	-0.03	-0.26	0.02	0.00	0.00	1.00	0.27	-0.03
$\lvert sw_{y3}\rvert$	0.03	0.03	0.03	0.02	0.11	0.04	0.30	0.62	0.01	0.01	-0.60	0.05	0.02	0.02	0.27	1.00	0.37
$\lvert sw_{y4}\rvert$	-0.02	-0.04	-0.01	0.00	0.17	0.10	-0.03	0.25	-0.01	0.02	-0.42	0.01	0.03	-0.03	-0.03	0.37	1.00

Fig. 14. Correlation matrix of the selected input parameters for the case #1 × 1 × 4_LF_RSP (all the parameters in absolute values are considered)

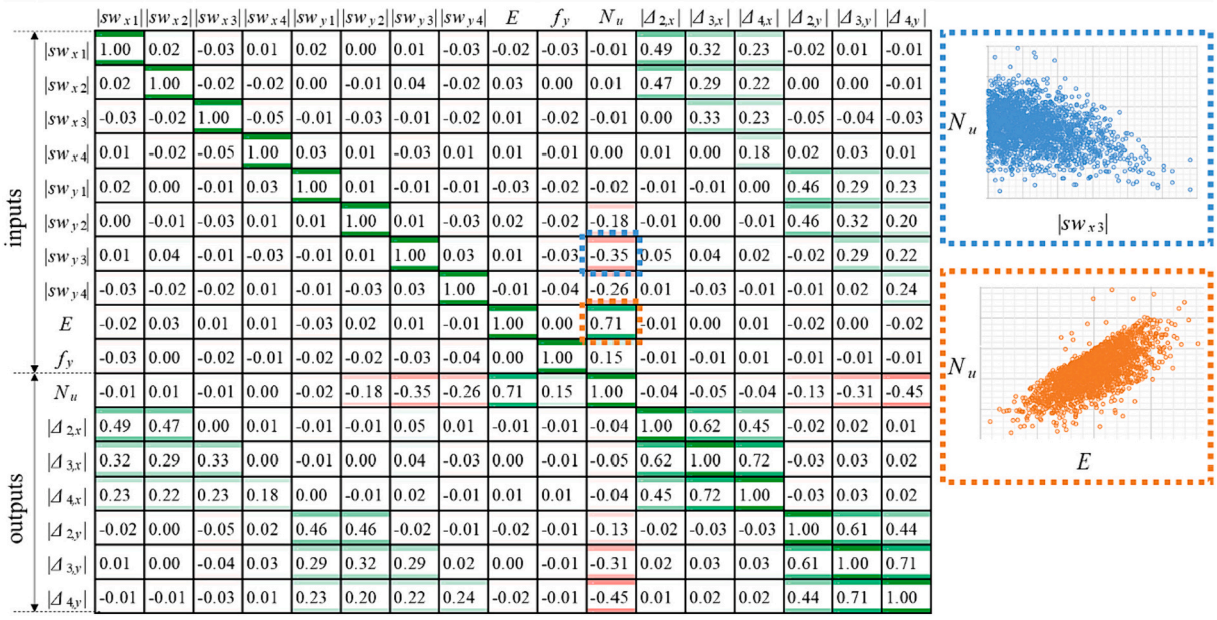

	$\lvert sw_{x1}\rvert$	$\lvert sw_{x2}\rvert$	$\lvert sw_{x3}\rvert$	$\lvert sw_{x4}\rvert$	$\lvert sw_{y1}\rvert$	$\lvert sw_{y2}\rvert$	$\lvert sw_{y3}\rvert$	$\lvert sw_{y4}\rvert$	E	f_y	N_u	$\lvert\Delta_{2,x}\rvert$	$\lvert\Delta_{3,x}\rvert$	$\lvert\Delta_{4,x}\rvert$	$\lvert\Delta_{2,y}\rvert$	$\lvert\Delta_{3,y}\rvert$	$\lvert\Delta_{4,y}\rvert$
$\lvert sw_{x1}\rvert$	1.00	0.02	-0.03	0.01	0.02	0.00	0.01	-0.03	-0.02	-0.03	-0.01	0.49	0.32	0.23	-0.02	0.01	-0.01
$\lvert sw_{x2}\rvert$	0.02	1.00	-0.02	-0.02	0.00	-0.01	0.04	-0.02	0.03	0.00	0.01	0.47	0.29	0.22	0.00	0.00	-0.01
$\lvert sw_{x3}\rvert$	-0.03	-0.02	1.00	-0.05	-0.01	-0.03	-0.01	-0.02	0.01	-0.02	-0.01	0.00	0.33	0.23	-0.05	-0.04	-0.03
$\lvert sw_{x4}\rvert$	0.01	-0.02	-0.05	1.00	0.03	0.01	-0.03	0.01	0.01	-0.01	0.00	0.01	0.00	0.18	0.02	0.03	0.01
$\lvert sw_{y1}\rvert$	0.02	0.00	-0.01	0.03	1.00	0.01	-0.01	-0.01	-0.03	-0.02	-0.02	-0.01	-0.01	0.00	0.46	0.29	0.23
$\lvert sw_{y2}\rvert$	0.00	-0.01	-0.03	0.01	0.01	1.00	0.01	-0.03	0.02	-0.02	-0.18	-0.01	0.00	-0.01	0.46	0.32	0.20
$\lvert sw_{y3}\rvert$	0.01	0.04	-0.01	-0.03	-0.01	0.01	1.00	0.03	0.01	-0.03	-0.35	0.05	0.04	0.02	-0.02	0.29	0.22
$\lvert sw_{y4}\rvert$	-0.03	-0.02	-0.02	0.01	-0.01	-0.03	0.03	1.00	-0.01	-0.04	-0.26	0.01	-0.03	-0.01	-0.01	0.02	0.24
E	-0.02	0.03	0.01	0.01	-0.03	0.02	0.01	-0.01	1.00	0.00	0.71	-0.01	0.00	0.01	-0.02	0.00	-0.02
f_y	-0.03	0.00	-0.02	-0.01	-0.02	-0.02	-0.03	-0.04	0.00	1.00	0.15	-0.01	-0.01	0.01	-0.01	-0.01	-0.01
N_u	-0.01	0.01	-0.01	0.00	-0.02	-0.18	-0.35	-0.26	0.71	0.15	1.00	-0.04	-0.05	-0.04	-0.13	-0.31	-0.45
$\lvert\Delta_{2,x}\rvert$	0.49	0.47	0.00	0.01	-0.01	-0.01	0.05	0.01	-0.01	-0.01	-0.04	1.00	0.62	0.45	-0.02	0.02	0.01
$\lvert\Delta_{3,x}\rvert$	0.32	0.29	0.33	0.00	-0.01	0.00	0.04	-0.03	0.00	-0.01	-0.05	0.62	1.00	0.72	-0.03	0.03	0.02
$\lvert\Delta_{4,x}\rvert$	0.23	0.22	0.23	0.18	0.00	-0.01	0.02	-0.01	0.01	0.01	-0.04	0.45	0.72	1.00	-0.03	0.03	0.02
$\lvert\Delta_{2,y}\rvert$	-0.02	0.00	-0.05	0.02	0.46	0.46	-0.02	-0.01	-0.02	-0.01	-0.13	-0.02	-0.03	-0.03	1.00	0.61	0.44
$\lvert\Delta_{3,y}\rvert$	0.01	0.00	-0.04	0.03	0.29	0.32	0.29	0.02	0.00	-0.01	-0.31	0.02	0.03	0.03	0.61	1.00	0.71
$\lvert\Delta_{4,y}\rvert$	-0.01	-0.01	-0.03	0.01	0.23	0.20	0.22	0.24	-0.02	-0.01	-0.45	0.01	0.02	0.02	0.44	0.71	1.00

Fig. 15. Correlation matrix of the selected input parameters for the case #1 × 1 × 4_LF_RSS (all the parameters are considered in the absolute values)

would be too large to plot, and also the values of these correlation were essentially very close to 0. Note: sw_1 is the abbreviation for the $sway_1$. Additionally, the parameter of the cumulative deviation of the 1st floor, Δ_1 is in the matter of mutual correlations the same as the sway parameter for the 1st floor, $sway_1$ (for each of the corresponding directions x or y, see also Fig. 1). Therefore, for the #RSP method (Fig. 14), only the input parameter Δ_1 is provided, and vice versa for the #RSS method (Fig. 15, Fig. 16), where $sway_1$ is provided. Linear correlations appeared to be sufficient enough to describe the mutual correlations, an examples of ant-hill plots for selected correlations are provided next to each matrix in these figures.

7. Discussion

7.1. Stochastic FORM approach and EC3 assumptions

From the results of the Table 3 and Fig. 10 it is evident, that such geometries of the steel frame might be established, where the ultimate resistance $N_{u,EN}$, determined in accordance with the EC3 assumptions [11] appears not to be conservative enough compared to the ultimate resistance determined by the more precise stochastic FORM method, $N_{u,FORM}$. The main reason of this is rather high correlation between the ultimate resistance N_u and the elastic Young's modulus E, as depicted e.g. in the correlation matrixes for the case #1 × 1 × 4_LF in the Fig. 14 – Fig. 16. The parameter E was for the FORM method considered as stochastic with mean value of 210 GPa and the coefficient of variation CoV = 5%. However, for the EC3 calculation, the standard procedure is to

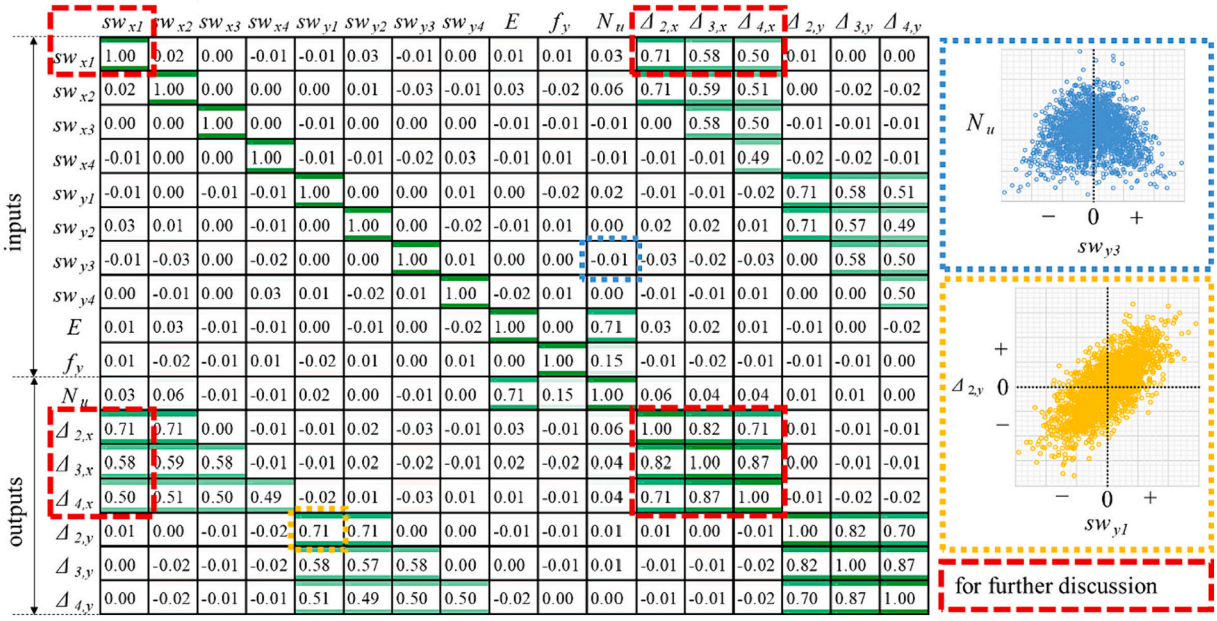

	sw_{x1}	sw_{x2}	sw_{x3}	sw_{x4}	sw_{y1}	sw_{y2}	sw_{y3}	sw_{y4}	E	f_y	N_u	$\Delta_{2,x}$	$\Delta_{3,x}$	$\Delta_{4,x}$	$\Delta_{2,y}$	$\Delta_{3,y}$	$\Delta_{4,y}$
sw_{x1}	1.00	0.02	0.00	-0.01	-0.01	0.03	-0.01	0.00	0.01	0.01	0.03	0.71	0.58	0.50	0.01	0.00	0.00
sw_{x2}	0.02	1.00	0.00	0.00	0.00	0.01	-0.03	-0.01	0.03	-0.02	0.06	0.71	0.59	0.51	0.00	-0.02	-0.02
sw_{x3}	0.00	0.00	1.00	0.00	-0.01	0.00	0.00	0.00	-0.01	-0.01	-0.01	0.00	0.58	0.50	-0.01	-0.01	-0.01
sw_{x4}	-0.01	0.00	0.00	1.00	-0.01	-0.01	-0.02	0.03	-0.01	0.01	-0.01	-0.01	-0.01	0.49	-0.02	-0.02	-0.01
sw_{y1}	-0.01	0.00	-0.01	-0.01	1.00	0.00	0.00	0.01	0.00	-0.02	0.02	-0.01	-0.01	-0.02	0.71	0.58	0.51
sw_{y2}	0.03	0.01	0.00	-0.01	0.00	1.00	0.00	-0.02	-0.01	0.01	0.00	0.02	0.02	0.01	0.71	0.57	0.49
sw_{y3}	-0.01	-0.03	0.00	-0.02	0.00	0.00	1.00	0.01	0.00	0.00	-0.01	-0.03	-0.02	-0.03	0.00	0.58	0.50
sw_{y4}	0.00	-0.01	0.00	0.03	0.01	-0.02	0.01	1.00	-0.02	0.01	0.00	-0.01	-0.01	0.01	0.00	0.00	0.50
E	0.01	0.03	-0.01	-0.01	0.00	-0.01	0.00	-0.02	1.00	0.00	0.71	0.03	0.02	0.01	-0.01	0.00	-0.02
f_y	0.01	-0.02	-0.01	0.01	-0.02	0.01	0.00	0.01	0.00	1.00	0.15	-0.01	-0.02	-0.01	-0.01	-0.01	0.00
N_u	0.03	0.06	-0.01	-0.01	0.02	0.00	-0.01	0.00	0.71	0.15	1.00	0.06	0.04	0.04	0.01	0.01	0.00
$\Delta_{2,x}$	0.71	0.71	0.00	-0.01	-0.01	0.02	-0.03	-0.01	0.03	-0.01	0.06	1.00	0.82	0.71	0.01	-0.01	-0.01
$\Delta_{3,x}$	0.58	0.59	0.58	-0.01	-0.01	0.02	-0.02	-0.01	0.02	-0.02	0.04	0.82	1.00	0.87	0.00	-0.01	-0.01
$\Delta_{4,x}$	0.50	0.51	0.50	0.49	-0.02	0.01	-0.03	0.01	0.01	-0.01	0.04	0.71	0.87	1.00	-0.01	-0.02	-0.02
$\Delta_{2,y}$	0.01	0.00	-0.01	-0.02	0.71	0.71	0.00	0.00	-0.01	-0.01	0.01	0.01	0.00	-0.01	1.00	0.82	0.70
$\Delta_{3,y}$	0.00	-0.02	-0.01	-0.02	0.58	0.57	0.58	0.00	0.00	-0.01	0.01	-0.01	-0.01	-0.02	0.82	1.00	0.87
$\Delta_{4,y}$	0.00	-0.02	-0.01	-0.01	0.51	0.49	0.50	0.50	-0.02	0.00	0.00	-0.01	-0.01	-0.02	0.70	0.87	1.00

Fig. 16. Correlation matrix of the selected input parameters for the case #1 × 1 × 4_LF_RSS (all the parameters are considered with the corresponding signs, plus or minus)

consider this material parameter by the mean value. For the FORM method, the decrease of the 0.1% quantile of the N_u is strongly affected by the stochastic values of the E modulus. In case of the EC3 approach, the "safety reserve" of these cases is then only on the side of considered loads.

From the analysed cases, the ultimate resistance based on EC3 assumptions appeared to be conservative only for #1 × 1 × 24_AF and #3 × 3 × 8_AF (see Table 3).

For the 24-floor frame of #1 × 1 × 24_AF, the EC3 resistance is $N_{u,EN}$ = 9.17 MN, and the values by the FORM are 9.67 MN or 10.89 MN for #RSS and #RSP methods respectively. The EC3 appears to be conservative enough with 5.2% or 15.8% reserve respectively. This is mainly due to the fact, that EC3 considers inclination of the whole structure in one direction – all the sways are defined by the same angle (Eq. 1), so called the "worst case" scenario. The more realistic initial imperfection considered in FORM method is not so overly conservative.

In case of the rather realistic frame geometry of the case #3 × 3 × 8_AF, the ultimate resistance based on EC3 is 50.7 MN, with FORM method of 51.1 MN (negligible difference in the #RSS and #RSP method). The value by EC3 appears to be rather realistic, only negligibly conservative with the reserve approximately 0.8%. For frame geometry #3 × 3 × 8_AF, the most significant linear correlation is observed between the N_u and the yield stress f_y, 0.72. Secondly, significant correlation is between N_u and E-modulus of 0.57, and a negative correlation of −0.14 between the N_u and the absolute value of input sway parameter sw_{y1} – the global imperfection of the first floor in the GCS y-direction (considering the correlation matrix for the #RSS method). Very similar values for correlation between N_u and f_y and between the N_u and E are in case of the #RSP method, 0.73 and 0.56 respectively. The whole matrix is not depicted due to size. These values explain the slightly more conservative resistance by EC3 method, as the resistance is predominantly dependent on the yield stress, which for the FORM calculations is considered with the mean value of 393.8 MPa (standard deviation of 22 MPa), and for the EC3 approach with the design value of 355 MPa. On the other hand, due to still significant dependence on the E modulus, the results by FORM are not too conservative (only 0.8% difference).

7.2. #RSS and #RSP methods for stochastic modelling of imperfections

In most cases, the differences in the ultimate resistances determined by FORM method using either #RSS or #RSP approach of the stochastic imperfection modelling are rather negligible (Table 3, **Fig. 11**). This statement will be probably valid only if the optimal correlation length L_{cor} is used to determine the initial correlation between the input storey deviations in case of the #RSP method. The workflow how to consider this optimal L_{cor} is described in the chapter 3.2.3, Eqs. 18–20. In case different L_{cor} is considered, the results of the #RSP approach might significantly deviate from the results by #RSS method, as shown in case of #1 × 1 × 4_LF_RSP, where the inputs of 0 m, 11.7 m and 999 m L_{cor} resulted in ultimate resistances of 3.98 MN, 4.56 MN and 4.88 MN respectively (see Table 3). However, if the optimal L_{cor} is considered, the difference between 4.56 MN and 4.62 MN (#RSP and #RSS method) is rather negligible. These various L_{cor} inputs have been tested only on this simple case, for the other cases, always only the optimal L_{cor} was used.

It is pointed out, that for certain geometries, for example structures with larger number of storeys, as 24-floor frame in case #1 × 1 × 24_AF, the difference in the ultimate resistance determined by FORM between the #RSS and #RSP approach might be more significant. The values for this case are 9.67 MN and 10.89 MN using the #RSS and #RSP method respectively, what is approximately 12% difference (more precisely 11.2 or 12.6%, depends which value is considered as the base value).

In general, the #RSS method is easier to use, as it does not require any input correlations. However, the #RSP method might be used for verification of the result for certain geometries, e.g. in case of frames with larger numbers of floors, under specific loading conditions, as in some cases, the #RSP method might have certain advantages to #RSS from the statistical "2 sigma rule" point of view [39]. Both methods are feasible to be used in case of stochastic analysis utilizing FORM method. Based on the provided results, it is expected, that larger differences in results between these two methods (considering the optimal L_{cor} is used for the #RSP) will be achieved for structures of larger number of stories, whereas for smaller number of stories, the differences are expected to be rather negligible.

7.3. Correlations between the parameters in the FORM method

The same pattern is being observed considering the correlation between ultimate resistance N_u and the other parameters for the #RSP and #RSS method (Fig. 14 and Fig. 15 respectively).

In case of the #RSP, the inputs are cumulative deviations $\Delta_{1,x} - \Delta_{4,x}$, and $\Delta_{1,y} - \Delta_{4,y}$, whereas the sways are considered as the outputs (are determined based on the input cumulative deviations) – the negative correlations between the N_u and the cumulative deviations in y direction (Δ_y) are increasing with the increasing floor number, being −0.08, −0.12, −0.27 and − 0.50 for the 1st, 2nd, 3rd and 4th floor respectively (Fig. 14). However, considering the sways, the largest influence on N_u is for the sway of the 3rd floor, −0.60. The same pattern in observed in case of #RSS, where the sways are the direct inputs, with the largest correlation of the 3rd floor sway equal to −0.35 (Fig. 15). The correlations between N_u and the cumulative deviations are also increasing for higher floors, as −0.02, −0.13, −0.31 and − 0.45 for the 1st to 4th floors respectively. These values might differ, as the #RSP method introduces certain correlations between the sways, whereas in the #RSS method, these correlations are 0 (Figs. 15, 16). On the other hand, the #RSS method with these 0 mutual correlations for the sway parameters resulted in certain correlations between the cumulative deviations (the values in red dashed frames in the Fig. 16). It is likely that these indirectly obtained correlations from the #RSS method would be feasible for utilization in case of the #RSP method, as a replacement of the correlations determined in accordance with the proposed workflow – Eqs. 18–20 and the optimal ω ratio values (Table 1). This however would probably result in the same problematic of the #RSS method, where the number of random realizations violating the cumulative tolerance criterion for the high floor number might decrease under 5% threshold too much (chapter 3.2.2.).

The mutual correlations of the other analysed frames are not depicted, as the patterns were rather similar to the provided example.

8. Summary

In this study, ultimate resistances of several steel frames of different geometries have been analysed, more precisely frames noted as: #1 × 1 × 1, #1 × 1 × 2, #1 × 1 × 3, #1 × 1 × 4, #1 × 1 × 24 and #3 × 3 × 8, where the notation of #x × y × z denotes the number of spans in the corresponding direction, e.g. #3 × 3 × 8 is an 8-storey steel frame with 3 spans in both horizontal directions. The loading of the frames was introduced in points of column-beam intersections, in all the floors "AF" variant, or only in the last uppermost floor, "LF" variant of loading. The summary of the analysed cases is in Table 3, and the geometries are depicted in the Figs. 2–7.

Advanced numerical analyses utilizing the finite element method (FEM) with consideration of geometrical and material nonlinearities and initial imperfections (so called GMNIA – geometrically and materially nonlinear imperfect analyses) have been conducted in order to obtain the ultimate resistance N_u of each frame.

Two approaches to estimate the ultimate resistance N_u were considered, first one in accordance with the European standard EC3 assumptions [11], where the input parameters are considered as deterministic. The obtained resistance is noted as $N_{u,EN}$. The second approach utilizes stochastic input parameters of the initial geometrical imperfections and material properties, along with the first order reliability method (FORM) from the EC0 standard [29]. Ultimate resistance is hence noted as $N_{u,FORM}$. The stochastic values of the initial geometrical imperfections, mean value and the standard deviation, are derived from the EN 1090–2:2018 [38] standard for execution of the steel structures. Based on the defined tolerance criteria of this standard, two methods to model the initial sway imperfections of the frame storeys are feasible, in this study noted as the #RSS (random storey sway) and #RSP (random storey position). The #RSS considers the sways of each i-th floor as random input $sway_i$ (or $\Delta_{dif,i,i-1}$), whereas in the #RSP method, the position of each floor relative to the base position Δ_i is the input (see Fig. 1). The point is, these inputs are derived from two different tolerance criteria, Eq. 15 and Eq. 16.

Both of these methods (#RSS and #RSP) are discussed in the chapter 3 of this study. The advantage of the #RSS is absence of the mutual correlation inputs for the sway imperfections, however it is questionable whether this would be suitable for larger number of floors (above circa 16th floor). The #RSP method requires input of the mutual correlations between the input storey deviations, making it less robust for usage, but might provide certain benefit for structures of larger number of floors. The recommended correlations for up to 24 floors, the ω ratio are obtained from the Table 1, based on the Eq. 19 and Eq. 20.

The differences in the ultimate resistances $N_{u,EN}$ and $N_{u,FORM}$ (determined utilizing the #RSS and #RSP methods) are summarized in the Table 3, and discussed. For majority of the model cases analysed in this study, the ultimate resistance in accordance with the EC3 [11] appeared to be larger than the more realistic resistance value determined by stochastic FORM method. The main reason of this was strong positive correlation between the resistance and the input elastic modulus of the steel material E. In case of the frame geometry #3 × 3 × 8, the EC3 resistance was only slightly more conservative, and for the rather unreal frame #1 × 1 × 24, the FORM method resulted in 5.4% and 18.7% larger resistances (using #RSS and #RSP methods respectively) then the $N_{u,EN}$ value.

In case the mutual correlations are input in accordance with the provisions of the chapter 3 of this document, the differences in results of $N_{u,FORM}$ with #RSS and #RSP method are rather negligible. The significant difference appeared in case of the 24 storey frame #1 × 1 × 24, approximately 12%. It is not excluded this difference might be larger in case structure of more storeys is being analysed. It is also assumed that diagonal bracing elements would be implemented for frame structures of large number of storeys. Hence the difference between the result by #RSS and #RSP method might be also smaller, as was in case of the frame #3 × 3 × 8.

The provisions for analogical numerical analyses of steel frame structures by FROM method are provided in this study, mainly for the #RSP method, where the definition of the mutual correlations between the random input parameters is required. These mutual correlations are expressed by the ω ratio (Eq. 19), which is summarized in the Table 1 for frames up to 24 equidistantly spaced floors.

The global numerical analysis of the whole steel structures with utilization of stochastic FORM approach might be useful as a replacement for multiple large-scale physical experiments which would be too costly. Alternatively, it might serve as a verification and helping tool of such large-scale experiments, as the full-scale blast test of three-story steel structure documented in a study by Hadjioannou et al. [62]. The advanced large-scale numerical models might be validated using these experimental data. Subsequently, stochastic methods might be introduced to estimate resistances with required reliability index. Or several variants of numerical models might be analysed, which might reduce the cost of multiple large-scale experimental studies.

9. Conclusion

This paper presents an examination of the ultimate resistance (N_u) of steel frames with varying geometrical configurations under loading scenarios that lead to compression in the columns. The core of the study lies in the adoption of the first-order reliability method (FORM), integrated with geometrically and materially nonlinear imperfect analyses (GMNIA), to assess the impact of stochastic methods on accounting for the randomness of initial imperfections in the 3D frame geometry. The research fills the gap in stochastic models of initial geometric imperfections of 3D frame structures.

Findings can be presented in several key points:

Stochastic Modelling Techniques: The authors proposed and compared two stochastic modelling techniques, Random Storey Sway

(RSS) and Random Storey Position (RSP), providing frameworks for modelling the random nature of initial imperfections. In both methods, the statistical values (mean and standard deviation) of the imperfections are derived from the tolerance criteria of the standard EN 1090–2:2018 [32]. While the RSS approach simplifies modelling by treating storey sway as an independent random variable, the RSP method integrates a correlation structure for positional deviations across floors, potentially offering a more detailed model of structural behaviour.

Numerical Analysis and Ultimate Resistance: Utilizing Advanced Latin Hypercube Sampling (ALHS), 2000 random realizations for each structural configuration underwent numerical analysis to determine their ultimate resistances ($N_{u,FORM}$), computed as the design quantile of random resistance. These ultimate resistance values $N_{u,FORM}$ were then compared with the deterministic $N_{u,EN}$ values derived from the EN 1993-1-1 standard.

Influence of Elastic Modulus (E): The correlation analysis showed that for slender column geometries, the elastic modulus (E) significantly affects N_u, exhibiting a strong positive correlation. The deterministic EC3 approach, which employs mean values for parameters such as E, was observed to yield slightly higher resistances in some instances compared to the more nuanced FORM method. This is attributed to the FORM method's inclusion of variability in E, leading to a more conservative estimate of N_u as it accounts for random realizations of E also below the mean value.

Comparison of Stochastic and Deterministic Methods: In seven frame geometries, the study found relatively small discrepancy between resistances obtained from stochastic and deterministic methods (maximally circa 15%). This suggests that, for these cases, the standard EC3 assumptions adequately reflect the crucial factors that govern structural resistance. Nonetheless, the FORM method's comprehensive nature, which encompasses material and geometric randomness, offers a finer gauge of structural reliability.

Enhanced Understanding of Structural Behaviour: The application of the FORM method has demonstrated its efficacy as an analytical tool for assessing ultimate resistance in the presence of geometrical imperfections. It enhances the understanding of the probabilistic nature of structural behaviour, providing a more realistic design approach compared to conventional deterministic methods. Findings from this study underline the importance of considering variability of material properties and geometric imperfections to achieve an economical and reliable design.

The findings of the study show the advantages of incorporating variability in material properties and geometric imperfections to achieve reliable structural designs. The use of stochastic methods, especially the FORM approach, offers valuable insights, supporting a more realistic design approach compared to traditional deterministic methods.

CRediT authorship contribution statement

Daniel Jindra: Writing – review & editing, Writing – original draft, Visualization, Validation, Methodology, Investigation, Formal analysis, Conceptualization. **Zdeněk Kala:** Writing – review & editing, Supervision, Project administration, Methodology, Funding acquisition, Conceptualization. **Jiří Kala:** Writing – review & editing, Supervision, Resources, Methodology, Data curation, Conceptualization.

Declaration of competing interest

The authors declare that they have no known competing financial interests or personal relationships that could have appeared to influence the work reported in this paper.

Data availability

Data will be made available on request.

Acknowledgements

This paper was created with the financial support of the Czech Science Foundation by project No.: 23−04712S “Importance of Stochastic Interactions in Computational Models of Structural Mechanics”.

References

[1] W. Liu, K.J.R. Rasmussen, H. Zhang, Y. Xie, Q. Liu, L. Dai, Probabilistic study and numerical modelling of initial geometric imperfections for 3D steel frames in advanced structural analysis, Structures 57 (2023) 105190, https://doi.org/10.1016/j.istruc.2023.105190.
[2] J. Melcher, Classification of structural steel members initial imperfections, in: Proc. of Structural Stability Research Council, Lehigh University, Bethlehem, 1980. https://scholarsmine.mst.edu/ccfss-library/234.
[3] Z. Kala, Sensitivity assessment of steel members under compression, Eng. Struct. 31 (2009) 1344–1348, https://doi.org/10.1016/j.engstruct.2008.04.001.
[4] S. Shayan, K.J.R. Rasmussen, H. Zhang, On the modelling of initial geometric imperfections of steel frames in advanced analysis, J. Constr. Steel Res. 98 (2014) 167–177, https://doi.org/10.1016/j.jcsr.2014.02.016.
[5] Y.H. He, G.Q. Li, J.Z. Zhang, B.H. Jiang, J. Zhang, Critical collapse deformation of 3-D steel frame with composite floor system, J. Constr. Steel Res. 208 (2023) 108034, https://doi.org/10.1016/j.jcsr.2023.108034.
[6] Y. Liu, Y.F. Zhu, W. Liang, H. Zhang, Y. Yao, Progressive collapse resistance and uncertainty analysis of post-tensioned steel frames, J. Constr. Steel Res. 208 (2023) 108007, https://doi.org/10.1016/j.jcsr.2023.108007.
[7] Y. Wang, B. Uy, D. Li, H.T. Thai, J. Mo, M. Khan, Behaviour and design of coupled steel-concrete composite wall-frame structures, J. Constr. Steel Res. 208 (2023) 107984, https://doi.org/10.1016/j.jcsr.2023.107984.
[8] J. Wang, K. Ke, M.C.H. Yam, M. Teng, W. Wang, Improving structural robustness of steel frame buildings by enhancing floor deck connections, J. Constr. Steel Res. 204 (2023) 107842, https://doi.org/10.1016/j.jcsr.2023.107842.
[9] G. Segura, I. Arrayago, E. Mirambell, Plastic redistribution capacity of stainless steel frames in fire, J. Constr. Steel Res. 208 (2023) 108019, https://doi.org/10.1016/j.jcsr.2023.108019.
[10] G. Segura, A. Pournaghshband, S. Afshan, E. Mirambell, Numerical simulation and analysis of stainless steel frames at high temperature, Eng. Struct. 227 (2021) 111446, https://doi.org/10.1016/j.engstruct.2020.111446.
[11] European Committee for Standardization, Part 1-1: General rules— General rules and rules for buildings, in: EN 1993-1-1:2005 Eurocode 3—Design of Steel Structures, European Committee for Standardization, Brussels, Belgium, 2005.
[12] S.L. Chan, H.Y. Huang, L.X. Fang, Advanced analysis of imperfect portal frames with semirigid base connections, J. Eng. Mech. 131 (6) (2005) 633–640, https://doi.org/10.1061/(ASCE)0733-9399(2005)131:6(633).
[13] R. Gonçalves, D. Camotim, On the incorporation of equivalent member imperfections in the in-plane design of steel frames, J. Constr. Steel Res. 61 (9) (2005) 1226–1240, https://doi.org/10.1016/j.jcsr.2005.01.006.
[14] M. Radwan, B. Kövesdi, Equivalent geometrical imperfections for local and global interaction buckling of welded square box section columns, Structures 48 (2023) 1403–1419, https://doi.org/10.1016/j.istruc.2023.01.045.
[15] M. Piątkowski, Experimental research on load of transversal roof bracing due to geometrical imperfections of truss, Eng. Struct. 242 (2021) 112558, https://doi.org/10.1016/j.engstruct.2021.112558.
[16] M.J. Clarke, R.Q. Bridge, G.J. Hancock, N.S. Trahair, Advanced analysis of steel building frames, J. Constr. St. Res. 23 (1–3) (1992) 1–29, https://doi.org/10.1016/0143-974X(92)90034-C.
[17] J.Y.R. Liew, W.F. Chen, H. Chen, Advanced inelastic analysis of frame structures, J. Constr. St. Res. 55 (2000) 245–265.
[18] Z. Kala, Modelling initial geometric imperfections of steel plane frames using entropy and eigenmodes, Int. J. Mech. 17 (2023) 64–73, https://doi.org/10.46300/9104.2023.17.10.
[19] Z. Kala, Strain energy and entropy based scaling of buckling modes, Entropy 25 (12) (2023) 1630, https://doi.org/10.3390/e25121630.
[20] R. Chacón, C. Pui-Polo, E. Real, TLS measurements of initial imperfections of steel frames for structural analysis within BIM-enabled platforms, Autom. Constr. 125 (2021) 103648, https://doi.org/10.1016/j.autcon.2021.103618.
[21] J.X. Gu, S.L. Chan, Second-order analysis and design of steel structures allowing for member and frame imperfections, Int. J. Numer. Methods Eng. 62 (5) (2005) 601–615.
[22] A. Agüero, I. Baláž, Y. Koleková, P. Martin, Assessment of in-plane behavior of metal compressed members with equivalent geometrical imperfection, Appl. Sci. 10 (22) (2020) 8174, https://doi.org/10.3390/app10228174.
[23] Z.P. Bažant, Y. Xiang, Postcritical imperfection-sensitive buckling and optimal bracing of large regular frames, J. Struct. Eng. 123 (4) (1997) 513–522, https://doi.org/10.1061/(ASCE)0733-9445(1997)123:4(513).
[24] A.R. Alvarenga, R.A.M. Silveria, Second-order plastic-zone analysis of steel frames – part II: effects of initial geometric imperfection and residual stress, Lat. Am. J. Solids Struct. 6 (4) (2009) 323–342.
[25] J.Y.R. Liew, D.W. White, W.F. Chen, Notional-load plastic-hinge method for frame design, J. Struct. Eng. ASCE 120 (5) (1994) 1434–1454.
[26] S.E. Kim, Practical Advanced Analysis for Steel Frame Design. [Ph.D. Thesis], Purdue University, West Lafayette, IN, 1996.

[27] A. Machowski, I. Tylek, Random equivalent initial bow and tilt in steel frame, Adv. Steel Constr. 8 (4) (2012) 383–397. ISSN: 1816-112X Available at: ascjournal.com/down/vol8no4/vol8no4_5.pdf.
[28] Y. Ding, X. Song, H.T. Zhu, Probabilistic progressive collapse analysis of steel-concrete composite floor systems, J. Constr. Steel Res. 129 (2017) 129–140, https://doi.org/10.1016/j.jcsr.2016.11.009.
[29] European Committee for Standardization, Basis of structural design, in: EN 1990: 2002 Eurocode 0, European Committee for Standardization, Brussels, Belgium, 2002.
[30] M.H. Faber, Statistics and probability theory, in: pursuit of Engineering Decision Support, (Part of the Topics in Safety, Risk, Reliability and Quality, book series TSRQ, volume 18), Springer Publishing Company, 2012, p. 192, eISBN: 978–94–007-4056-3, https://doi.org/10.1007/978-94-007-4056-3.
[31] Y.G. Zhao, T. Ono, A general procedure for first/second-order reliability method (FORM/SORM), Struct. Saf. 21 (1999) 95–112.
[32] Z. Kala, From probabilistic to quantile-oriented sensitivity analysis: new indices of design quantiles, Symmetry 12 (10) (2020) 1720, https://doi.org/10.3390/sym12101720.
[33] Z. Kala, Sensitivity analysis in probabilistic structural design: a comparison of selected techniques, Sustainability 12 (11) (2020) 4788, https://doi.org/10.3390/su12114788.
[34] Z. Kala, New importance measures based on failure probability in global sensitivity analysis of reliability, Mathematics 9 (19) (2021) 2425, https://doi.org/10.3390/math9192425.
[35] J. Jönsson, M.S. Müller, Ch. Gamst, J. Valeš, Z. Kala, Investigation of European flexural and lateral torsional buckling interaction, J. Constr. Steel Res. 156 (2019) 105–121, https://doi.org/10.1016/j.jcsr.2019.01.026.
[36] Ansys, Inc, ANSYS 19.0, Ansys, Inc, Canonsburg, PA, USA, 2018.
[37] D. Chen, Y. Zhang, H. Qian, H. Wang, X. Jin, Numerical approach for simulating the tensioning process of complex prestressed cable-net structures, J. Civ. Eng. Manag. 27 (8) (2021) 571–578, https://doi.org/10.3846/jcem.2021.15776.
[38] British Standard Institution (BSI): BS EN 1090–2:2018: Execution of steel structures and aluminium structures Part 2: Technical requirements for steel structures. ISBN 978 0 580 89588 3.
[39] D. Jindra, Z. Kala, J. Kala, Two stochastic methods to model initial geometrical imperfections of steel frame structures, Buildings 14 (1) (2024) 196, https://doi.org/10.3390/buildings14010196.
[40] Z. Kala, Reliability analysis of the lateral torsional buckling resistance and the ultimate limit state of steel beams with random imperfections, J. Civ. Eng. Manag. 21 (7) (2015) 902–911, https://doi.org/10.3846/13923730.2014.971130.
[41] Z. Kala, J. Valeš, J. Jönsson, Random fields of initial out of straightness leading to column buckling, J. Civ. Eng. Manag. 23 (7) (2017) 902–913, https://doi.org/10.3846/13923730.2017.1341957.
[42] Z. Kala, Stability problems of steel structures in the presence of stochastic and fuzzy uncertainty, Thin-Walled Struct. 45 (2007) 861–865.
[43] D. Jindra, Z. Kala, J. Kala, Flexural buckling of stainless steel CHS columns: reliability analysis utilizing FEM simulations, J. Constr. Steel Res. 188 (2022) 107002, https://doi.org/10.1016/j.jcsr.2021.107002.
[44] D. Jindra, Z. Kala, J. Kala, Buckling curves of stainless steel CHS members: current state and proposed provisions, J. Constr. Steel Res. 198 (2022) 107521, https://doi.org/10.1016/j.jcsr.2022.107521.
[45] Z. Kala, Sensitivity and reliability analysis of lateral-torsional buckling resistance of steel beams, Arch. Civ. Mech. Eng. 15 (4) (2015) 1098–1107, https://doi.org/10.1016/j.acme.2015.03.007.
[46] J. Lindner, R. Gietzelt, Imperfektionsannahmen für Stützenschiefstellungen (assumptions for imperfections for out-of-plumb of columns), Stahlbau 53 (4) (1984) 97–102.
[47] D. Jindra, Z. Kala, J. Kala, Ultimate load capacity of multi-story steel frame structures with geometrical imperfections: A comparative study of two methods, Modern Building Materials, Structures and Techniques. MBMST 2023. Lecture Notes in Civil Engineering, vol. 392. Springer, Cham. doi:https://doi.org/10.1007/978-3-031-44603-0_15.
[48] T. Sakai, M. Nakajima, K. Tokaji, N. Hasegawa, Statistical distribution patterns in mechanical and fatigue properties of metallic materials, J. Soc. Mater. Sci. 46 (6) (1997) 63–74, https://doi.org/10.2472/jsms.46.6Appendix_63.
[49] Z. Sekulski, Statistical properties of the yield strength of normal strenhth hull structural steel plates, in: The Annals of "Dunarea de Jos" 42, University of Galati, Fascicle XI, Shipbuilding, 2019, https://doi.org/10.35219/AnnUGalShipBuilding.2019.42.08.
[50] M. De Stefano, R. Nudo, G. Sara, S. Viti, Effects of randomness in steel mechanical properties on rotational capacity of RC beams, Mater. Struct. 34 (2001) 92–99, https://doi.org/10.1007/BF02481557.
[51] M. Muskulus, S. Schafhirt, Reliability-based design of wind turbine support structures, in: Symposium on Reliability of Engineering System, SRES'2015, Hangzhou, China, 2015, https://doi.org/10.13140/RG.2.1.5125.5766.
[52] I. Arrayago, K.J.R. Rasmussen, E. Real, Statistical analysis of the material, geometrical and imperfection characteristics of structural stainless steels and members, J. Const. Steel Res. 175 (2020) 106378, https://doi.org/10.1016/j.jcsr.2020.106378.
[53] Cross-Section Properties, www.staticstools.eu/en/ Accessed 27 Oct. 2023.
[54] D.E. Hungtington, C.S. Lyrintzis, Improvements to and limitations of Latin hypercube sampling, Prob. Eng. Mech. 13 (4) (1998) 245–253, https://doi.org/10.1016/S0266-8920(97)00013-1.
[55] M.D. McKay, R. Beckman, W. Conover, A comparison of three methods for selecting values of input variables in the analysis of output from a computer code, Technometrics 21 (2) (1979) 239–245, https://doi.org/10.1080/00401706.1979.10489755.
[56] R.L. Iman, W.J. Conover, A distribution-free approach to inducing rank correlation among input variables, Commun. Stat. Simul. Comput. 11 (3) (1982) 311–334, https://doi.org/10.1080/03610918208812265.
[57] Dynardo GmbH, OptiSLang software manual: Methods for multi-disciplinary optimization and robustness analysis, in: Weimar, 2019. https://www.ansys.com/products/platform/ansys-optislang.
[58] K. Pearson, X. On the criterion that a given system of deviations from the probable in the case of a correlated system of variables is such that it can be reasonably supposed to have arisen from random sampling, The London, Edinburgh and Dublin Philosophical Mag. J. Sci. Series 5 50 (302) (1900) 157–175, https://doi.org/10.1080/14786440009463897.
[59] T.W. Anderson, D.A. Darling, A test of goodness-of-fit, J. Am. Stat. Assoc. 49 (268) (1954) 765–769, https://doi.org/10.1080/01621459.1954.10501232.
[60] W.W. Daniel, Applied Nonparametric Statistics, 2nd ed., Duxbury, Pacific Grove, CA, 1990. ISBN 978–0–534-91976-4.
[61] N. Smirnov, Table for estimating the goodness of fit of empirical distributions, Ann. Math. Stat. 19 (2) (June, 1948) 279–281, https://doi.org/10.1214/aoms/1177730256.
[62] M. Hadjioannou, A.E. McKay, P.C. Benshoof, Full-scale blast tests on a conventionally designed three-story steel braced frame with composite floor slabs, Vibration 4 (4) (2021) 865–892, https://doi.org/10.3390/vibration4040049.